AIR FORCE INSTITUTE OF TECHNOLOGY

AIR UNIVERSITY
UNITED STATES AIR FORCE

EFFECT OF VIBRATION ON THE HEAT TRANSFER RATE FROM CYLINDERS IN FREE CONVECTION IN AIR

THESIS

GAM/ME/66B-10

Leon H. Chaffee
Major USAF

SCHOOL OF ENGINEERING

WRIGHT-PATTERSON AIR FORCE BASE, OHIO

AFLC-WPAFB-SEP 65 6M

GAM/ME/66B-10

EFFECT OF VIBRATION ON THE HEAT TRANSFER RATE FROM CYLINDERS IN FREE CONVECTION IN AIR

THESIS

Presented to the Faculty of the School of Engineering of

Air Force Institute of Technology

Air University

in Partial Fulfillment of the

Requirements for the Degree of

Master of Science

DISTRIBUTION OF THIS
DOCUMENT IS UNLIMITED

by

Leon H. Chaffee, B. S.

Major USAF

Graduate Aerospace-Mechanical Engineering

June 1966

Preface

This report is concerned with the effects of vibration on convective heat transfer rates. I hope it will add some small contribution to the world of knowledge and be of some use in future studies of the subject. The research itself has been time consuming yet interesting, at times exasperating yet not without personal satisfaction. My one regret is the lack of time with which to follow up on the unexpected.

I wish to express my appreciation to Dr. Andrew J. Shine, Head, Department of Mechanical Engineering, Air Force Institute of Technology. Not only did he assist me in selecting this particular project, but as my thesis advisor he gave me timely and invaluable suggestions. Mr. John Flahive and Mr. Richard Brown provided vital assistance and solved many pratical problems associated with the assembly of equipment. Finally, I wish to thank Mr. Millard Wolfe, Foreman of the school shops, for his assistance and interest without which this project could not have been completed.

Leon H. Chaffee

Table of Contents

List of Figures

List of Symbols

a	Amplitude of vibration - in
D	Outside diameter of cylinder - ft
E	Voltage drop across cylinder - volts
f	Frequency of vibration - cps
h	Local coefficient of heat tranfer - B/hr ft^2F
I	Current through cylinder - amps
k_f	Thermal conductivity of air at t_f - B/hr ft F
Nu	Nusselt number, hD/k_f - dimensionless
Pr	Prandtl number - dimensionless
Re	Reynolds number of vibration, $4afD/\nu_f$ - dimensionless
t_a	Temperature at ambient air - F
t_f	Temperature of boundary layer fluid, $(t_a + t_w)/2$ - F
t_w	Temperature of cylinder wall - F
ν_f	Kinematic viscosity of air at t_f - ft^2/sec

Abstract

This study is a follow-on investigation of the effects of sinusoidal vibration on the heat transfer rate from cylinders in free convection in air. The purpose was to obtain and correlate heat transfer data in the region of the critical Reynolds number, to investigate the effect of the vibration at higher Reynolds numbers through the use of a larger diameter cylinder, and to obtain Schlieren photographs of the boundary layer in the vicinity of the critical Reynolds number. Three stainless steel cylinders with 0.12 in, 0.25 in, and 0.75 in diameters were vibrated at frequencies from 10 to 50 cycles per second, at amplitudes from 0.0185 to 0.765 inches, and at surface-to-ambient temperature potentials of 50F, 100F, and 200F. Results show that each cylinder displays a similar characteristic pattern progressing from a region in which the heat transfer rate is independent of vibration, through a transition region, to a region where the heat transfer rate generally parallels the recommended forced convection curve of McAdams and is a function only of the vibration intensity. An increased frequency shifts the transition region in the direction of higher vibration intensities. Schlieren photographs show a considerable increase in turbulence in the boundary layer through the transition region.

I. Introduction

Background

In a free convective environment, the heat transfer rate from a body to its surrounding is determined by the mechanism in the boundary layer. In order to increase the heat transfer rate, the boundary layer must be altered by reducing its thickness or increasing the transverse fluid movement in the boundary layer or both. Vibration is one method of producing increased transverse fluid motion. A knowledge of the influence of vibrations on the rate of heat transfer by free convection from a heated surface would be of considerable interest to the design engineer. Unfortunately, to date there is a limited knowledge concerning the physical mechanisms of the processes involved.

A number of studies have been conducted over the past two decades in order to ascertain transverse vibration effects on the convective heat transfer rate from both flat plates and cylinders. Two of the more recent studies involved the use of sinusoidal vibration, a method of vibration not used previously.

In 1962, Shine and Jarvis investigated the sinusoidal vibration effects on the convective heat transfer rate from heated cylinders in air. They mounted the test cylinder horizontally with the ends rigidly clamped. The cylinder, excited near one end, was vibrated at its resonant frequency in a sinusoidal wave form in the vertical plane. Cylinders of 0.032 in and 0.072 in diameter were vibrated from 15 to 75 cycles per second and at amplitudes of from 0.002 to 0.99 in (Ref 4:2).

In 1965, Watson conducted an extension of the work of Shine and Jarvis to investigate the effects of sinusoidal vibration at higher vibration Reynolds numbers (based on the average vibration velocity 4af and cylinder diameter), at two selected surface-to-ambient temperature potentials, and at different positions along the cylinder. Cylinders of 0.072 in, 0.12 in, and 0.25 in diameter were vibrated from 16 to 80 cycles per second and at amplitudes of from 0.05 to 1.5 in. He obtained a maximum vibration Reynolds number of 1100 with the 0.25 in diameter cylinder (Ref 5:3).

From the studies conducted to date the following summary of conclusions were made (Ref 3:3, 4:2, 5:2):

a. The heat transfer rate was independent of the direction of transverse vibration (horizontal or vertical).

b. Below a critical vibration intensity (af), the heat transfer rate was unaffected by vibration.

c. Above a critical vibration intensity the heat transfer rate increased with the increased vibration intensity and was a function only of the vibration intensity.

d. At high vibration intensities, the effect of vibration was independent of temperature and the heat transfer rate generally paralleled the recommended forced convection curve of McAdams.

e. The heat transfer rate was independent of the position of the test point along the sinusoidally vibrated cylinder and only dependent on the vibration intensity at the position.

Purpose

The purpose of this study was to extend the investigation of the effect of sinusoidal vibration on the convective heat transfer rate from heated cylinders to air. The specific objectives were (1) to obtain and correlate heat transfer data in the region of the critical vibration Reynolds number (dimensionless vibration intensity) with the same size cylinders as Watson used; (2) to investigate the effect at higher Reynolds numbers through the use of a larger diameter cylinder and a redesign of the vibrating apparatus to accommodate the larger cylinder; and (3) to obtain Schlieren photographs of the boundary layer and surrounding fluid in the region of the critical Reynolds number.

II. Apparatus

The apparatus used in this study consisted basically of (1) three electrically heated circular test cylinders, (2) a vibrating assembly into which a cylinder was clamped, (3) a protective enclosure to seclude the cylinder from random convective air currents, (4) a photographic arrangement used to determine vibration amplitude, and (5) a Schlieren apparatus.

Test Cylinders

The test cylinders were 42 to 46 in long sections of polished, stainless steel, thin-walled tubing with 0.12 in, 0.25 in, and 0.75 in outside diameters. Heat was provided by passing adjustable direct electrical current through the cylinder. An internally attached iron-constantan thermocouple permitted instantaneous monitoring of the cylinder wall temperature at the test position, the point of maximum vibration amplitude.

Vibrating Assembly

Two different vibrating assemblies were used during the course of this study. The first, used with the 0.12 in and 0.25 in diameter cylinders, was the same assembly used by Watson (Ref 5:5). The cylinder was rigidly clamped at both ends. An electromagnetic vibrator was positioned directly below the cylinder and six inches from the left end clamp. Variable frequency and amplitude vibrations were transmitted to the cylinder through the vibrator drive rod which also served to constrain vibratory motion to the vertical plane. A schematic diagram of this assembly is shown in Figure 1. An adjustable but constant axial tension was applied to the cylinder at its right end to permit selected variation in the natural response frequency of the cylinder and to compensate for thermal expansion. The second vibrating assembly, used with the 0.25 in and 0.75 in diameter cylinders, was designed to accommodate the greater forces required to vibrate the larger diameter cylinders. The clamps were pinned to allow rotation in the vertical plane. The vibrator drive rod was connected to a moment arm extension of the right cylinder clamp. Constraint of vibratory motion to the vertical plane was effected both through the pinned clamp arrangement and through increased clamp size. A schematic diagram of this assembly is shown in Figure 2. Axial tension for this assembly was applied to the left end of the cylinder.

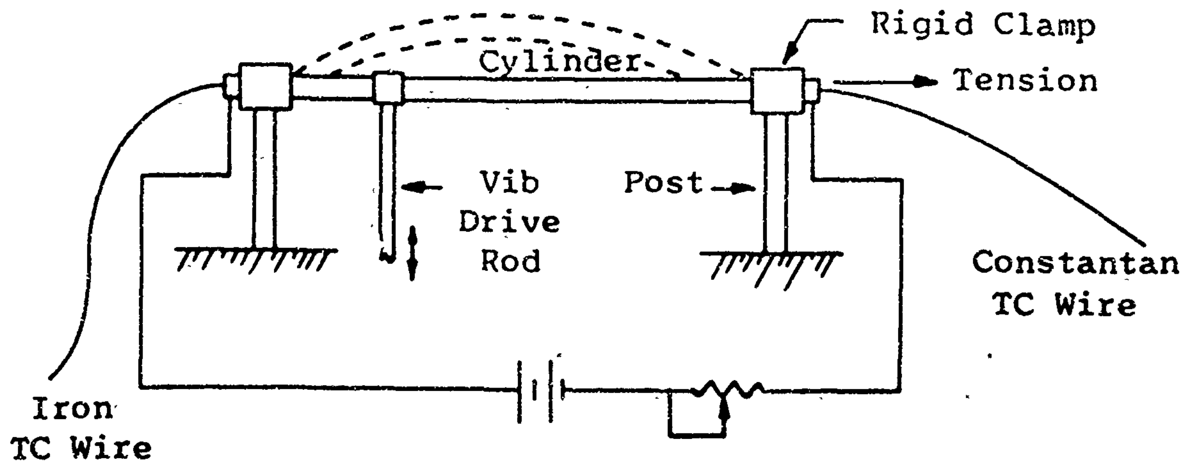

Figure 1

Schematic of Watson Vibrating Assembly

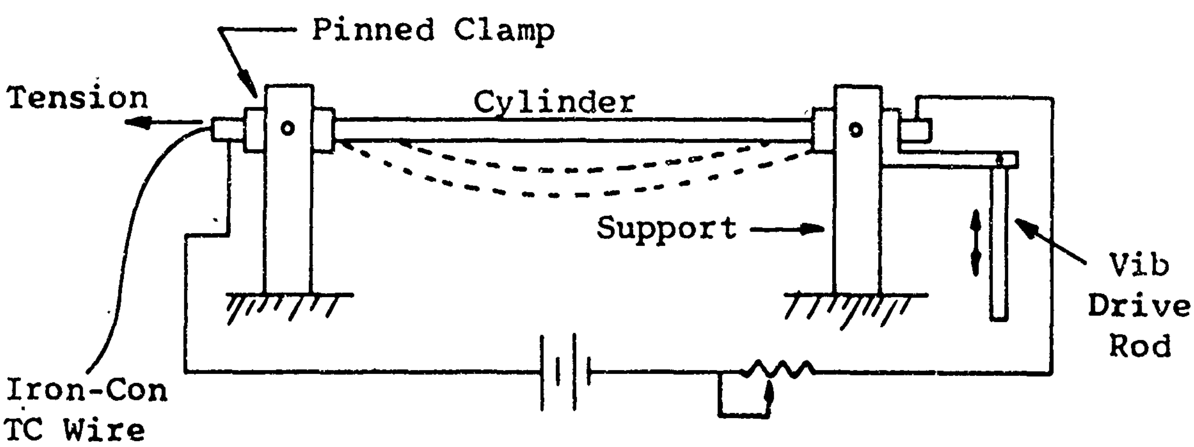

Figure 2

Schematic of Improved Vibrating Assembly

Enclosure

The test cylinder with its associated clamps and clamp supports of the Watson assembly was mounted in a 48 x 12 x 30 in enclosure. For the improved assembly, the enclosure dimension were 60 x 20 x 30 in. In each case the top and bottom were vented to permit free convection around the cylinder. An iron-constantan thermocouple was located within each enclosure at cylinder level to sense ambient temperature.

Photograph Arrangement

A parallel light beam was passed through a glass window in the front panel of the enclosure, across the test cylinder, and through a 1/32 in wide slit in the rear panel. The resulting shadow of the vibrating test cylinder was then directed onto a rotating mirror which swept it across the open aperture to a Polaroid camera. The resulting photograph provided a measureable amplitude of vibration. A schematic diagram of the photographic arrangement is shown in Figure 3. For the Schlieren photographs the slit was removed and a spark lamp provided the open aperture time for the photograph.

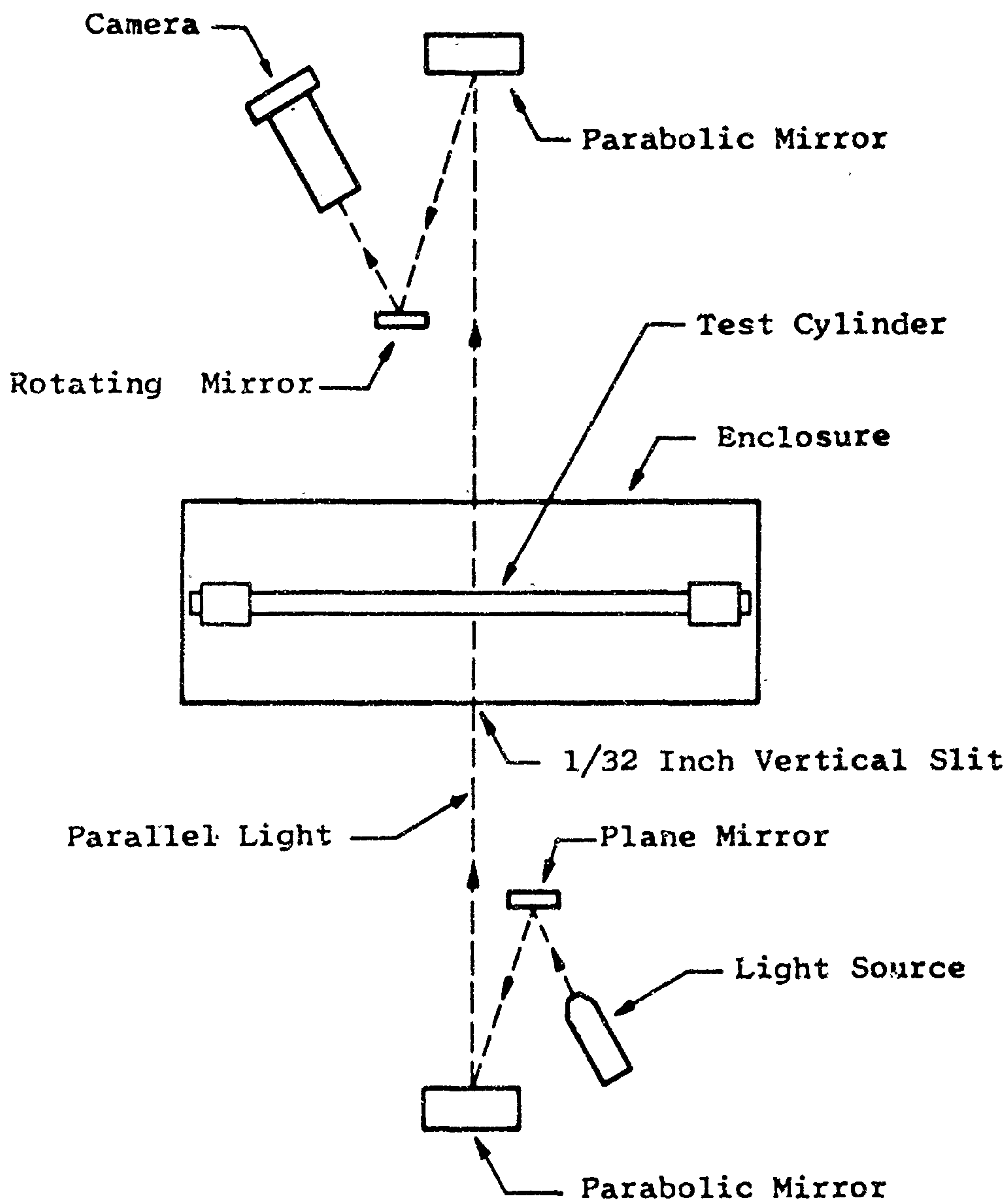

Figure 3

Schematic of Photographic Arrangement
for Measuring Vibration Amplitude

III. Experimental Procedure

The test cylinder was initially heated without vibration to one of the following arbitrarily chosen temperature potentials: 50F, 100F, 200F. The total electrical power EI delivered to the cylinder was then determined by recording the metered values of the current I and the voltage drop E. A photograph of the static cylinder was taken to determine the scale factor for subsequent vibrational amplitude measurements. The temperature potential and power measurements provided data for determining the free convective heat transfer rate.

The cylinder was then vibrated at its response frequency at incremental increases in amplitude. The frequency and amplitude measurements provided data for determining the vibration Reynolds number. This procedure was continued until a decrease in temperature potential was noted indicating an increase in the heat transfer rate. From this point on the power delivered to the cylinder was increased incrementally and the amplitude of vibration adjusted until the temperature potential had stablized at the originally chosen value. Recordings of the power delivered to the cylinder, temperature potential, and frequency of vibration were made and a photograph of the vibrating cylinder was taken for each adjusted change in amplitude. This procedure was continued for a series of test runs during which the temperature potential was maintained at the originally chosen value. The double amplitude of vibration 2a was determined for each photograph using a microscopic comparator graduated to 0.0001 in. The experimental ranges were as follows: frequency f, 10 to 50 cps; amplitude a, 0.0185 to 0.765 in.

The maximum error in the determination of the Reynolds number arising from measurements of a and f was quite large at extremely low Reynolds numbers; however, above a Reynolds number of 75 the range of error was generally from two to five per cent. The maximum error in the determination of the heat transfer coefficient, expressed as the Nusselt number Nu, arising from measurements of temperature potential $t_w - t_a$, I, and E was calculated to be 7.1 per cent. As the values of Re and Nu increased the associated error decreased.

Schlieren photographs of the 0.75 in diameter cylinder heated to a temperature potential of 200F were taken at selected intervals through the entire sequence of data obtained for that temperature potential.

IV. Results

The results of this study are presented in Figures 4 through 7. Heat tranfer coefficients are expressed as Nusselt numbers and vibration intensities are expressed as Reynolds numbers.

There exist for each cylinder (1) a region at low vibration intensities in which vibration has no effect on the heat transfer rate; (2) a region at higher vibration intensities in which the variation in the heat transfer coefficient generally parallels the recommended forced convection curve of McAdams; and (3) a characteristic transition region in between.

There is conclusive evidence that the rate of heat transfer in the transition region is not a function of vibration intensity alone. Data presented in Figures 4 and 5 for temperature potentials of 92F and 100F show that an increase in vibration frequency shifts the transition region in the direction of higher vibration intensities.

Although the variation of the heat transfer coefficient with vibration intensity results in the same basic pattern for each cylinder size tested, in the region where the variation generally parallels the curve of

McAdams there does exist an increase in displacement from this curve with increased cylinder size. This is shown in Figures 4 through 7.

At the higher vibration intensities, the variation in the heat transfer coefficient with vibration intensity for a given cylinder size is independent of the temperature potential and solely a function of the vibration intensity. This is shown in Figure 6.

The Schlieren photographs of the 0.75 in diameter cylinder at a temperature potential of 100F are presented in Figures 13 through 19.

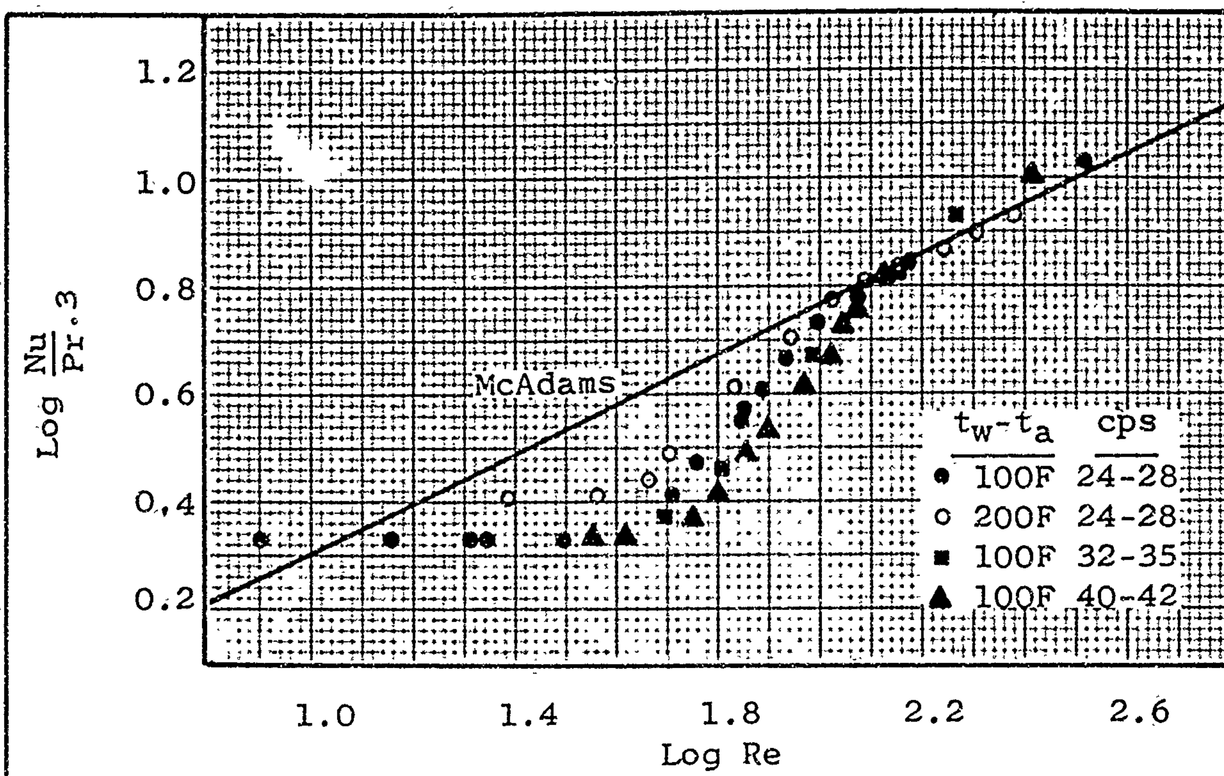

Figure 4

Variation of the Heat Transfer Coefficient with Vibration Intensity for the 0.12 in Diameter Test Cylinder

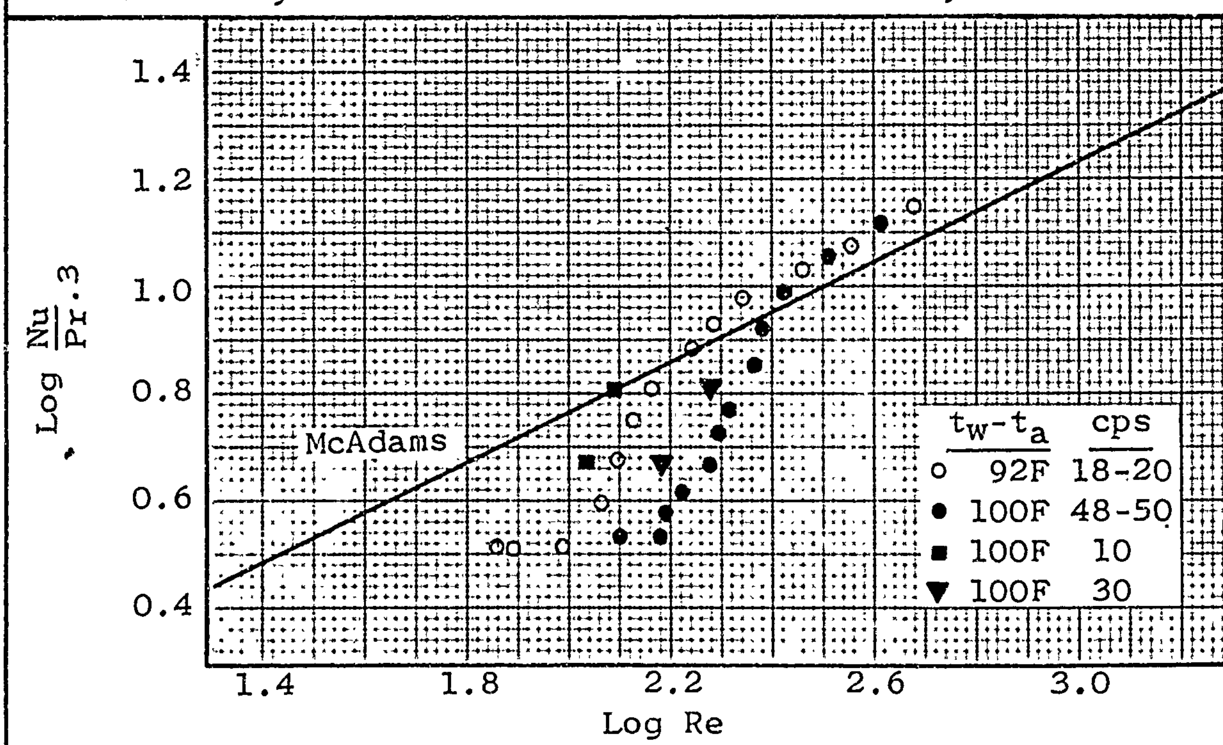

Figure 5

Variation of the Heat Transfer Coefficient with Vibration Intensity at Selected Vibration Frequencies for the 0.25 in Diameter Test Cylinder

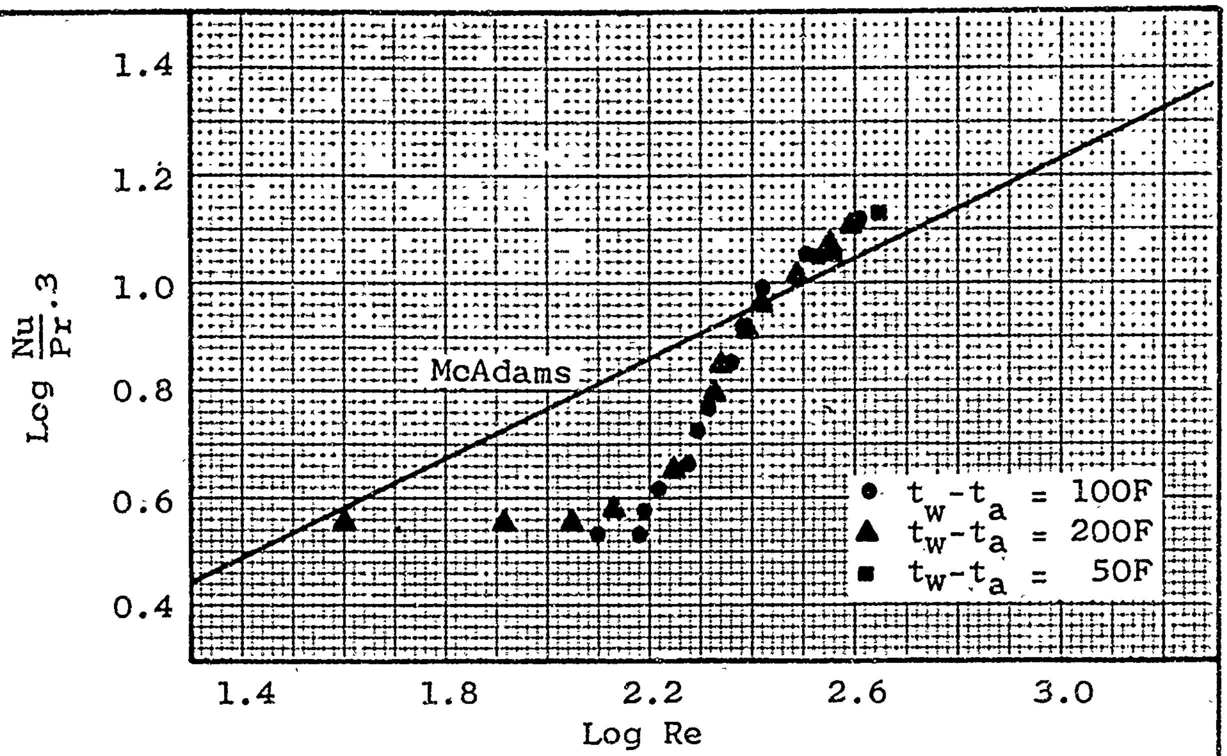

Figure 6

Variation of the Heat Transfer Coefficient with Vibration Intensity at Selected Temperature Potentials of the 0.25 in Diameter Test Cylinder

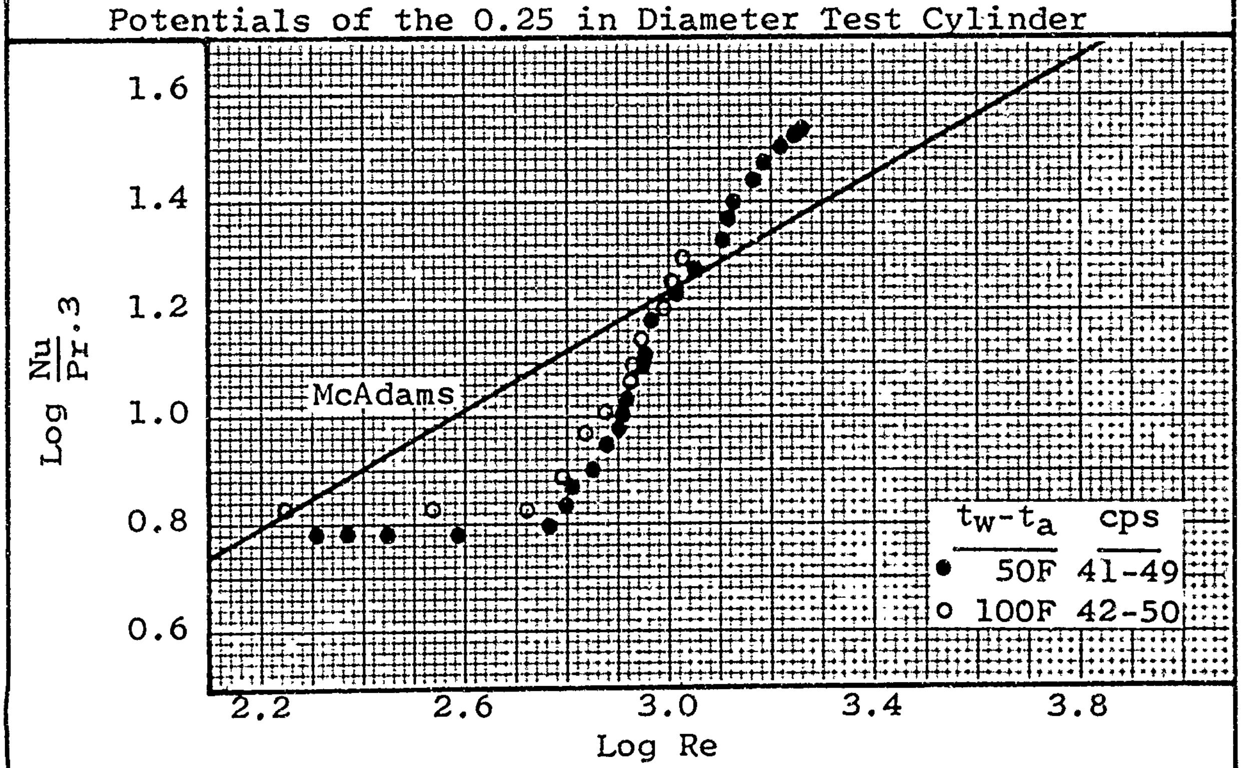

Figure 7

Variation of the Heat Transfer Coefficient with Vibration Intensity for the 0.75 in Diameter Test Cylinder

V. Discussion of Results

Figure 8 shows the variation of the heat transfer coefficient with vibration intensity at similar vibration frequencies for the three cylinders tested during this study. Each curve has a similar characteristic pattern. Below a critical vibration Reynolds number the heat transfer rate is independent of the vibration intensity. Above this Reynolds number the heat transfer rate increases markedly through the transition region as the vibration intensity is increased. At still higher vibration intensities the heat transfer rate follows a curve that generally parallels the recommended forced convection curve of McAdams. The displacement of the heat transfer rate curve from the curve of McAdams in this parallel region increases as the cylinder diameter is increased.

Results obtained with the 0.12 in diameter cylinder are compared in Figure 9 to those obtained by Watson for the same size cylinder. Correlation is not satisfactory since Watson does not show the same characteristic transition pattern. Examination of the experimental data by Watson revealed that his initial Nusselt number (no vibration) is 25 per cent higher than the free convection value recommended by McAdams for the cylinder diameter

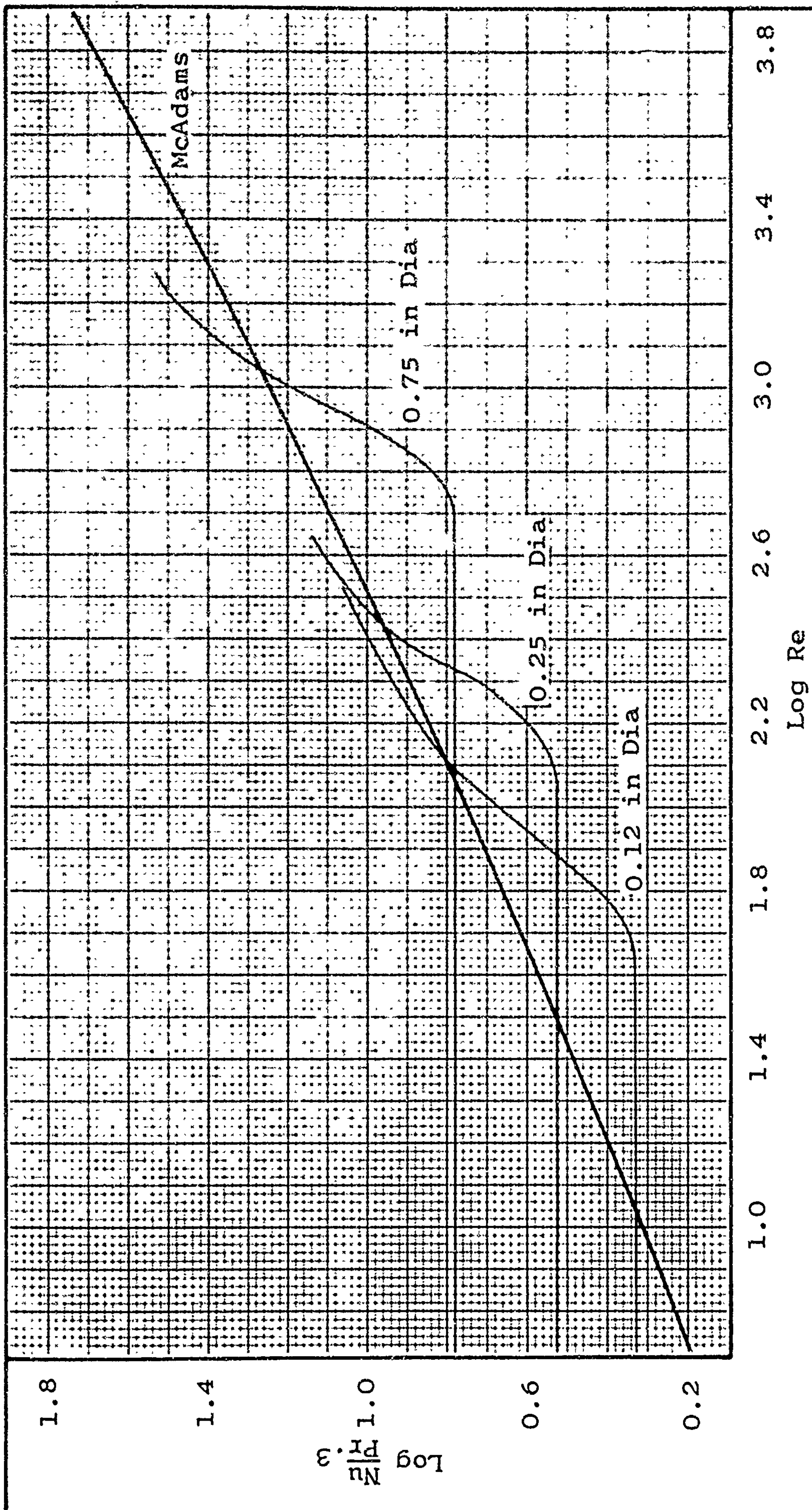

Figure 8

Comparison of the Variation of the Heat Transfer Coefficient with Vibration Intensity for the 0.12, 0.25, and 0.75 in Diameter Test Cylinders, f = 40-50 cps and temperature potential involved (Ref 2:176). Consequently, the data obtained by Watson is questionable. The initial Nusselt number obtained in this study deviates from that recommended by McAdams by five per cent.

In Figure 10 the results of this study with those of Watson and Neely for the 0.25 in diameter cylinder are compared. Again, correlation with Watson is unsatisfactory at the lower vibration Reynolds numbers. For this cylinder, the initial Nusselt number he obtained is 19 per cent higher than the recommended McAdams value; therefore, his data is again questionable. The initial Nusselt number obtained in this study deviates from the recommended McAdams value by one per cent. Correlation with Neely, on the other hand, is excellent; the difference in the paths through the transition region can be attributed to different frequencies of vibration. This is brought out more clearly in Figure 11 which shows that the transition region moves toward lower vibration intensities as the frequency is decreased.

An additional significance of the excellent correlation with Neely is the indication that the variation of the local heat transfer coefficient with

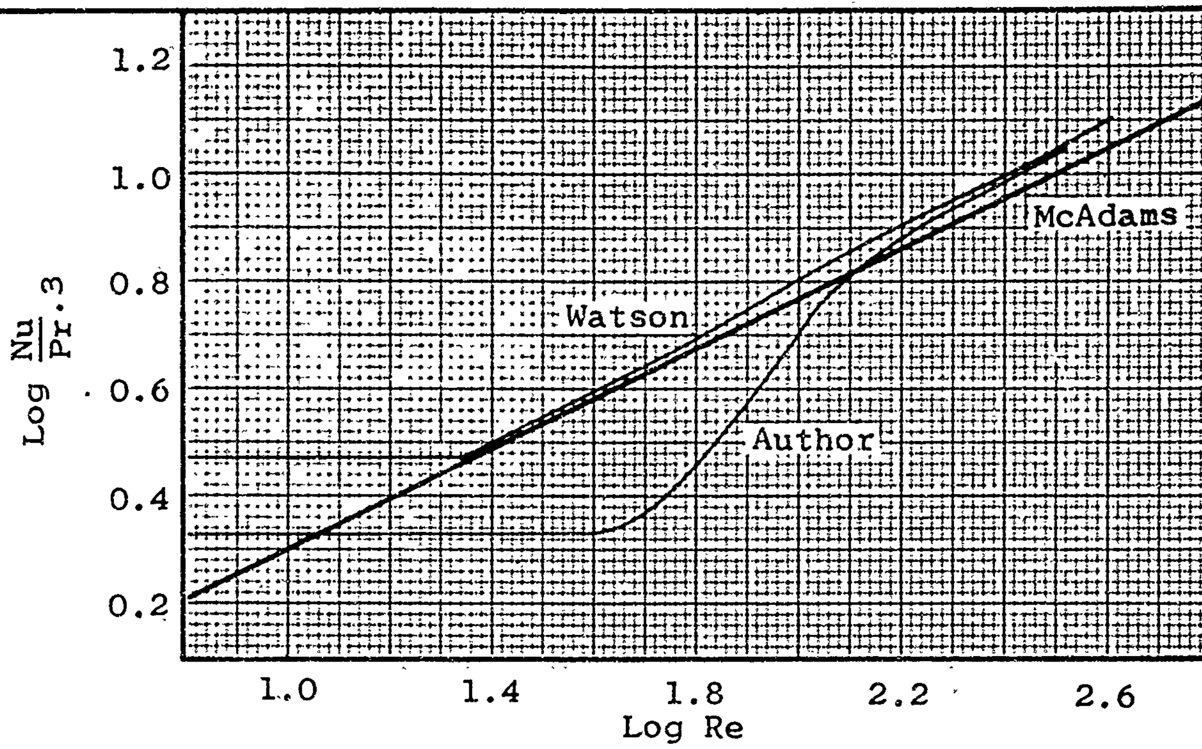

Figure 9

Comparison of Results for the
0.12 in Diameter Test Cylinder

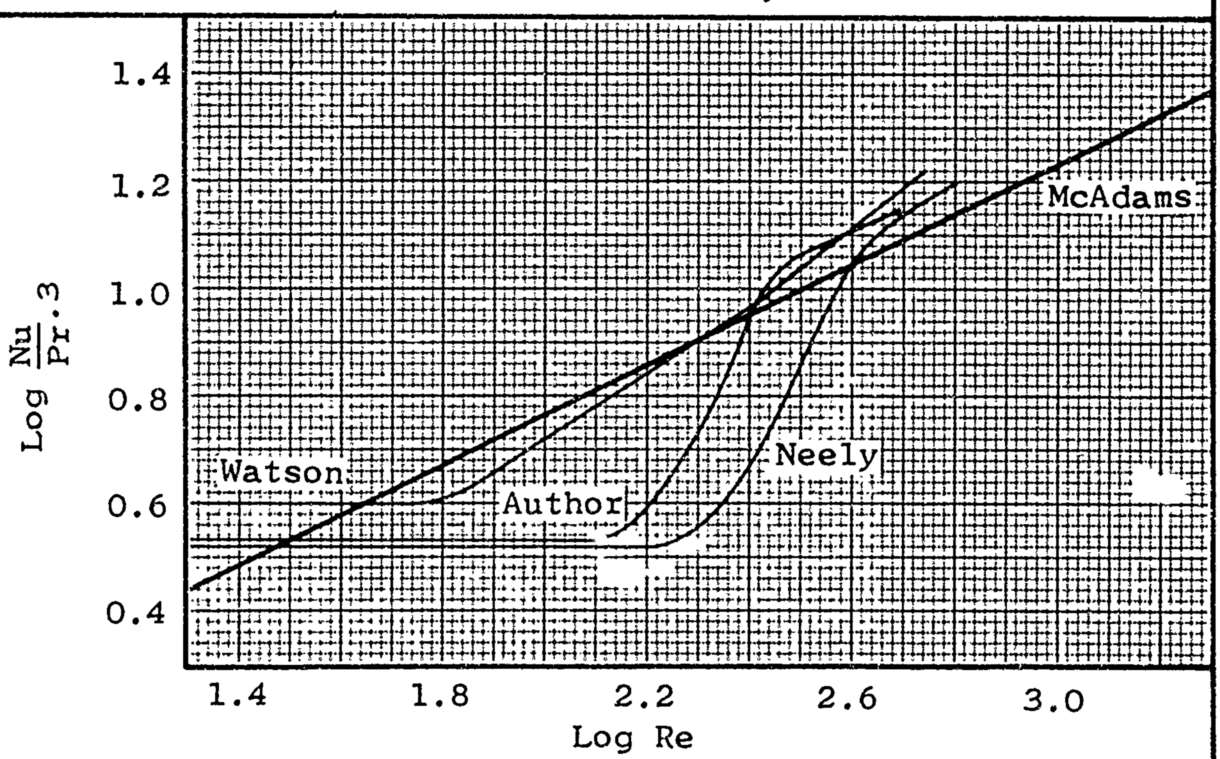

Figure 10

Comparison of Results for the 0.25 in
Diameter Test Cylinder, $t_w - t_a$ = 90F to 100F

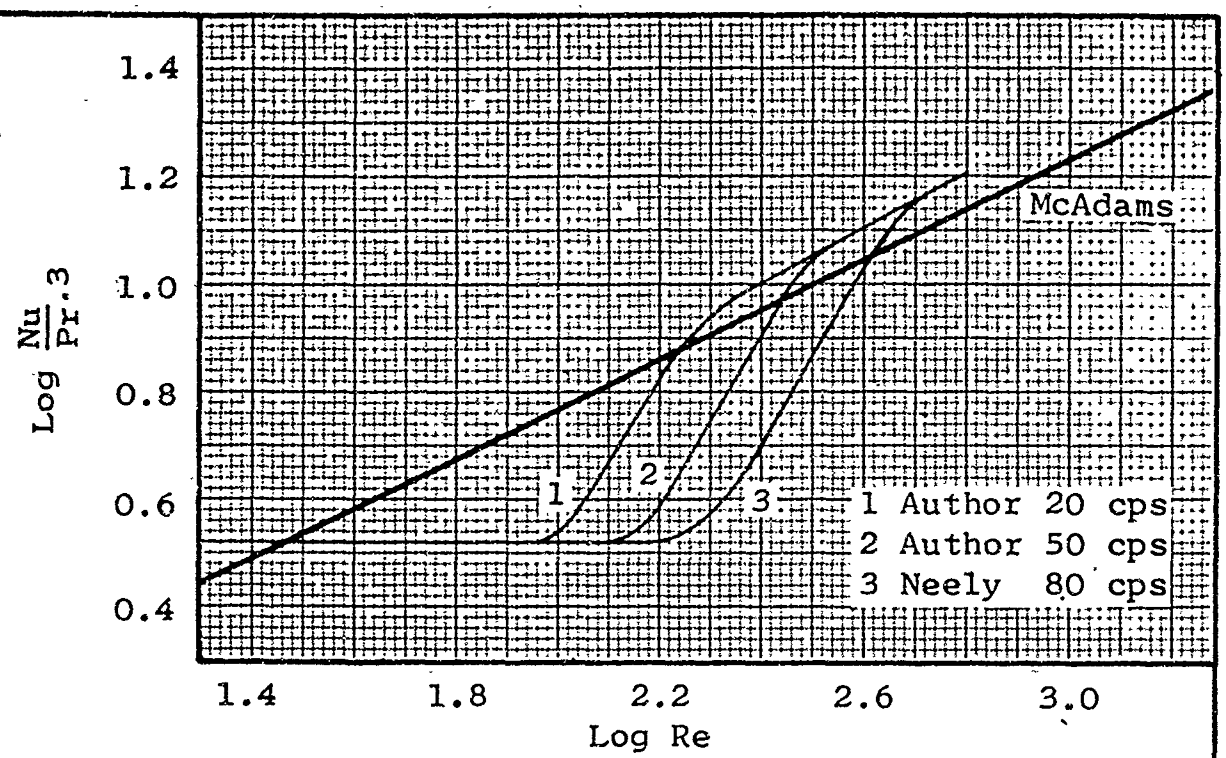

Figure 11

Effect of Frequency on the Variation of the Heat Transfer Coefficient with Vibration Intensity for the 0.25 in Diameter Test Cylinder, $t_w - t_a$ = 90F to 100F

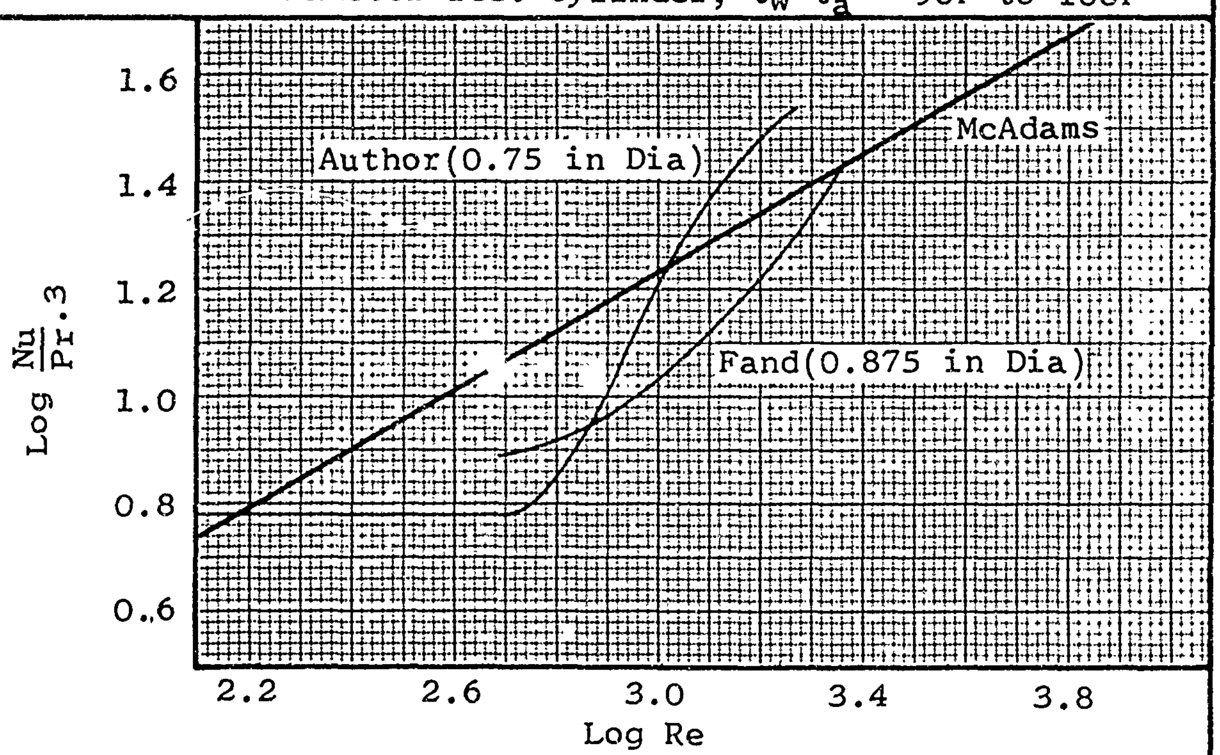

Figure 12

Comparison of Results for the 0.75 in Diameter Test Cylinder, $t_w - t_a$ = 50F vibration intensity does not depend upon the method of vibration used. The method of vibration used by Neely was not sinusoidal as was used in this study. He vibrated the entire cylinder transversely in the horizontal plane.

Figure 12 shows a comparison of the test results obtained with the 0.75 in diameter cylinder in this study and the 0.875 in diameter cylinder by Fand and Kaye (Ref 1:495). Although direct correlation is not possible since the cylinders are of different size, the general transition patterns appear similar. Unfortunately, Fand and Kaye were not able to obtain data at higher vibration intensities to show the region generally paralleling the recommended curve of McAdams. Fand and Kaye show a slightly different curvature through the transition region which might be explained by the fact that their data was obtained using higher and variable frequencies, 54 to 225 cycles per second, rather than using constant frequencies as in this study (Ref 1:494).

The results of this study show that for a given vibration frequency there is a given path for the variation of the heat transfer coefficient through the transition region. The supposition here is that the overall effect is a function of vibration frequency when in reality it may be a function of vibration amplitude. In either case it is apparent that the variation of the heat transfer coefficient through the transition region is not soley a function of the vibration intensity, but is indeed more complex. Additional qualitative study of this phenomenon is needed.

Figure 8 shows an increase in displacement from the recommended curve of McAdams with increased cylinder diameter. A critical examination of the results obtained in this study and those obtained by Neely indicate that the variation of the heat transfer coefficient with vibration intensity above the transition region may not parallel the curve of McAdams but rather may be constantly diverging from it. Further qualitative study is needed to investigate the behavior of this possible divergence, particularly in the gap between the 0.25 in and 0.75 in diameter cylinders.

The Schlieren photographs show a dramatic increase in vortex turbulence in the boundary layer as the vibration intensity is increased through the transition region. This increase in turbulence provides ample justification for the rapid increase in the heat transfer rate with increased vibration intensity through the transition region.

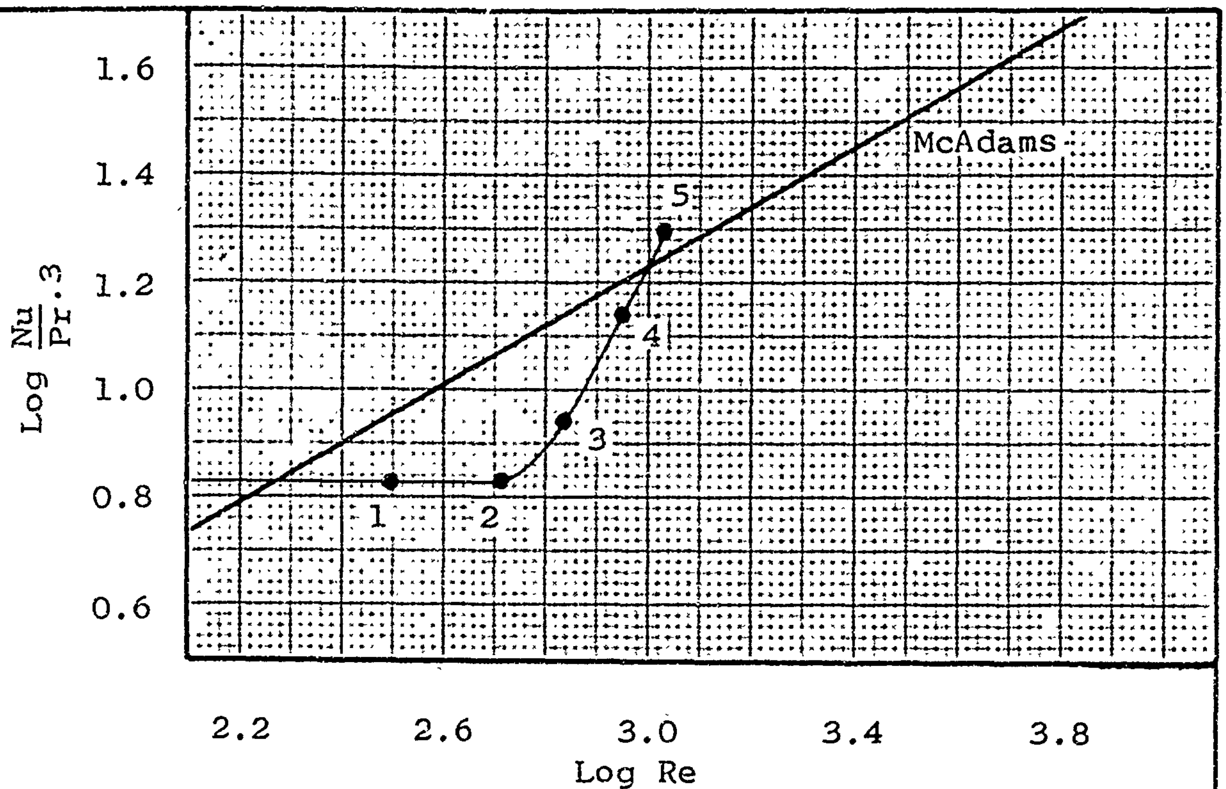

Figure 13

Positions Where Schlieren Photographs Were Taken of the 0.75 in Diameter Test Cylinder, $t_w - t_a$ = 100F

Figure 14

Schlieren Photograph of Static 0.75 in Diameter Test Cylinder, $t_w - t_a = 100F$

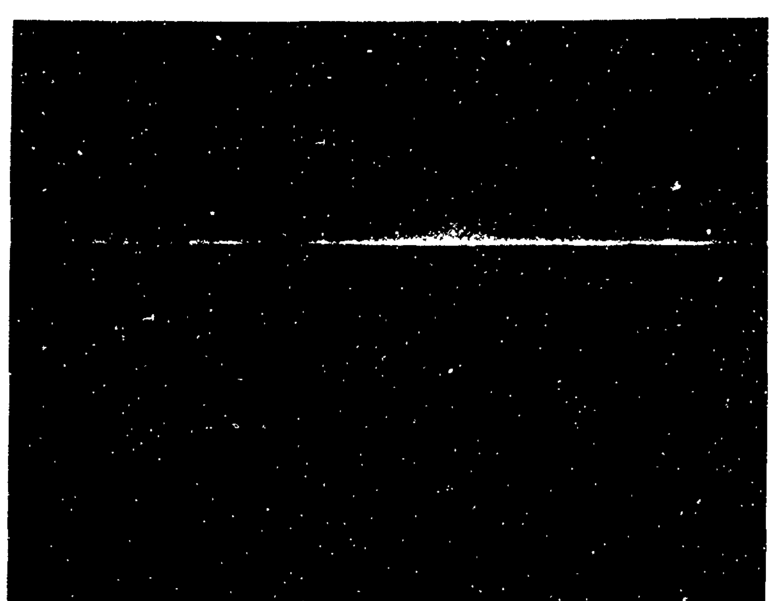

Figure 15

Schlieren Photograph at Position 1

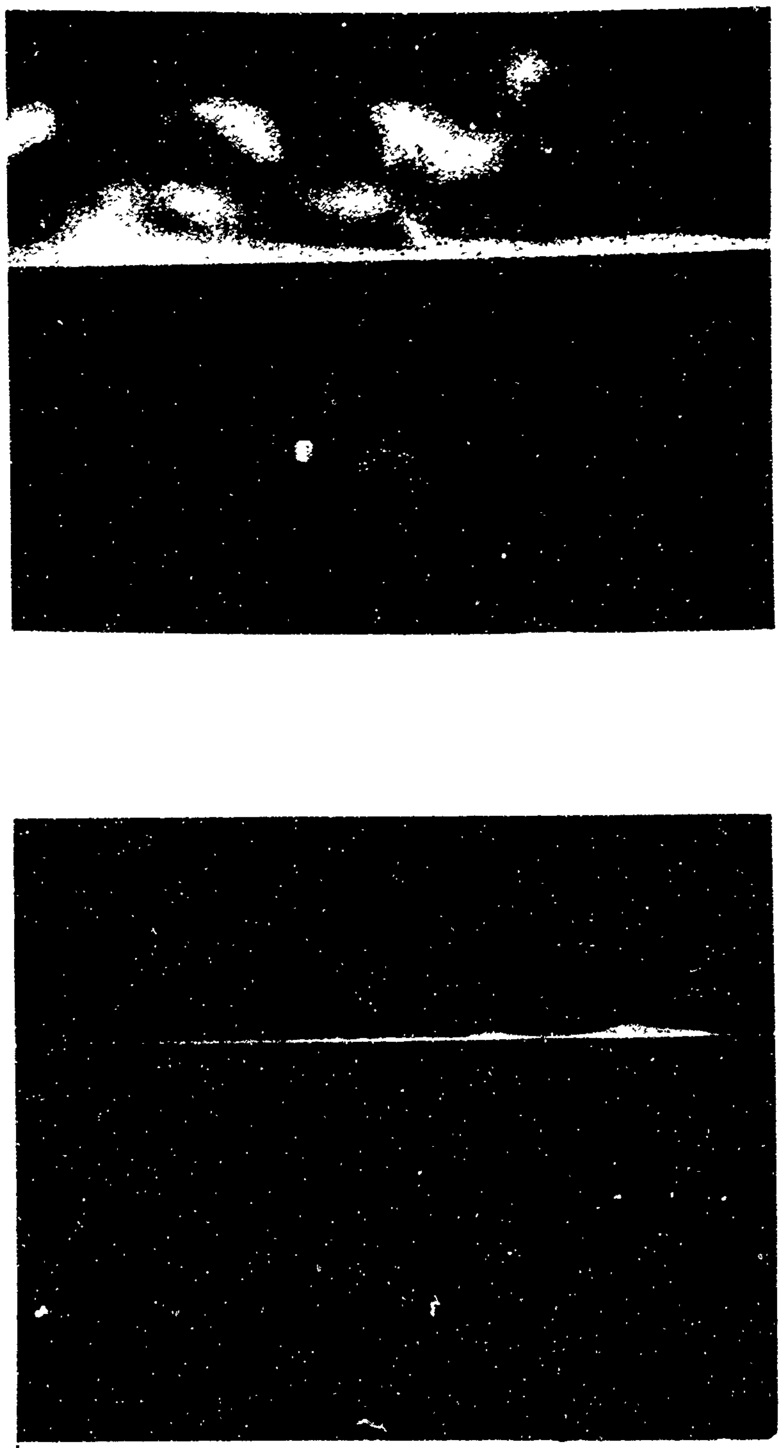

Figure 16

Schlieren Photographs at Position 2

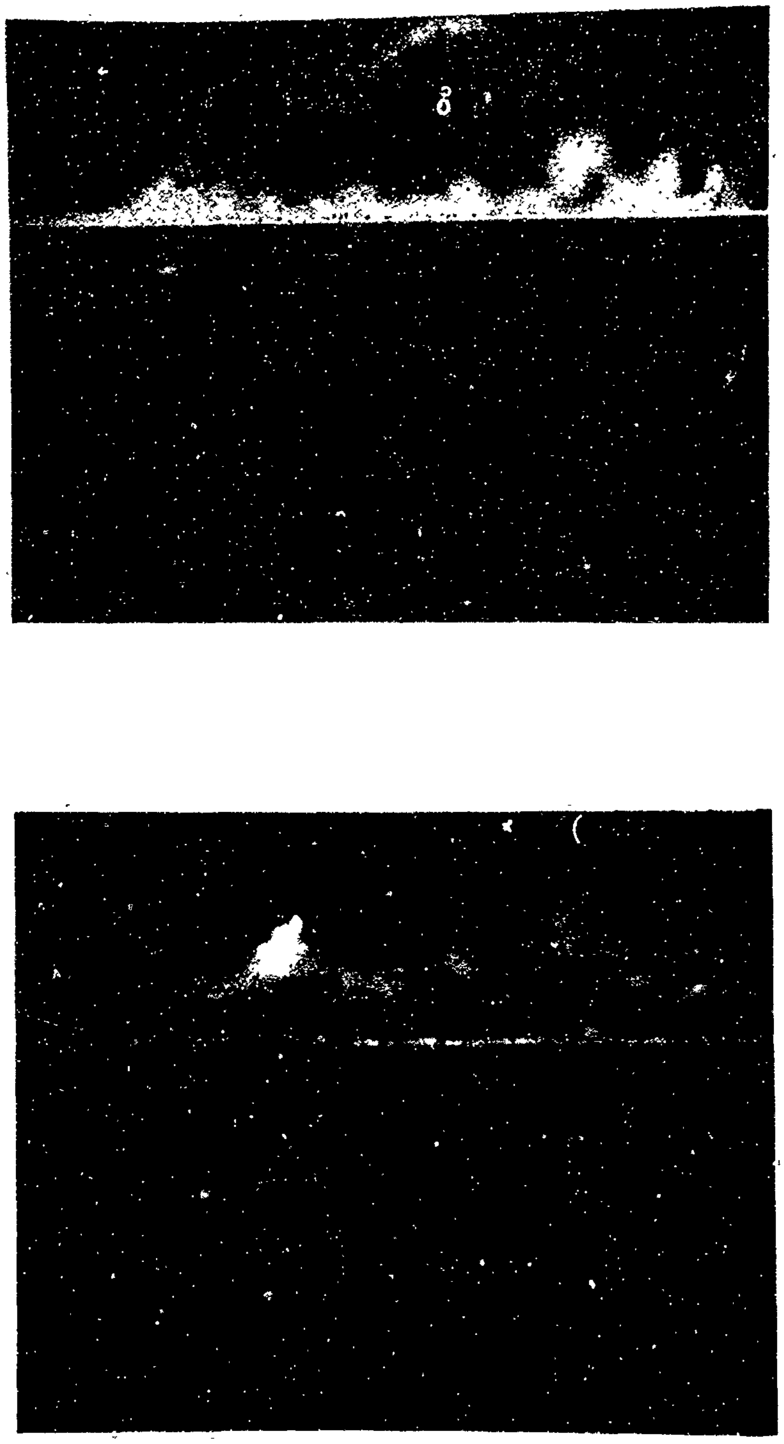

Figure 17

Schlieren Photographs at Position 3

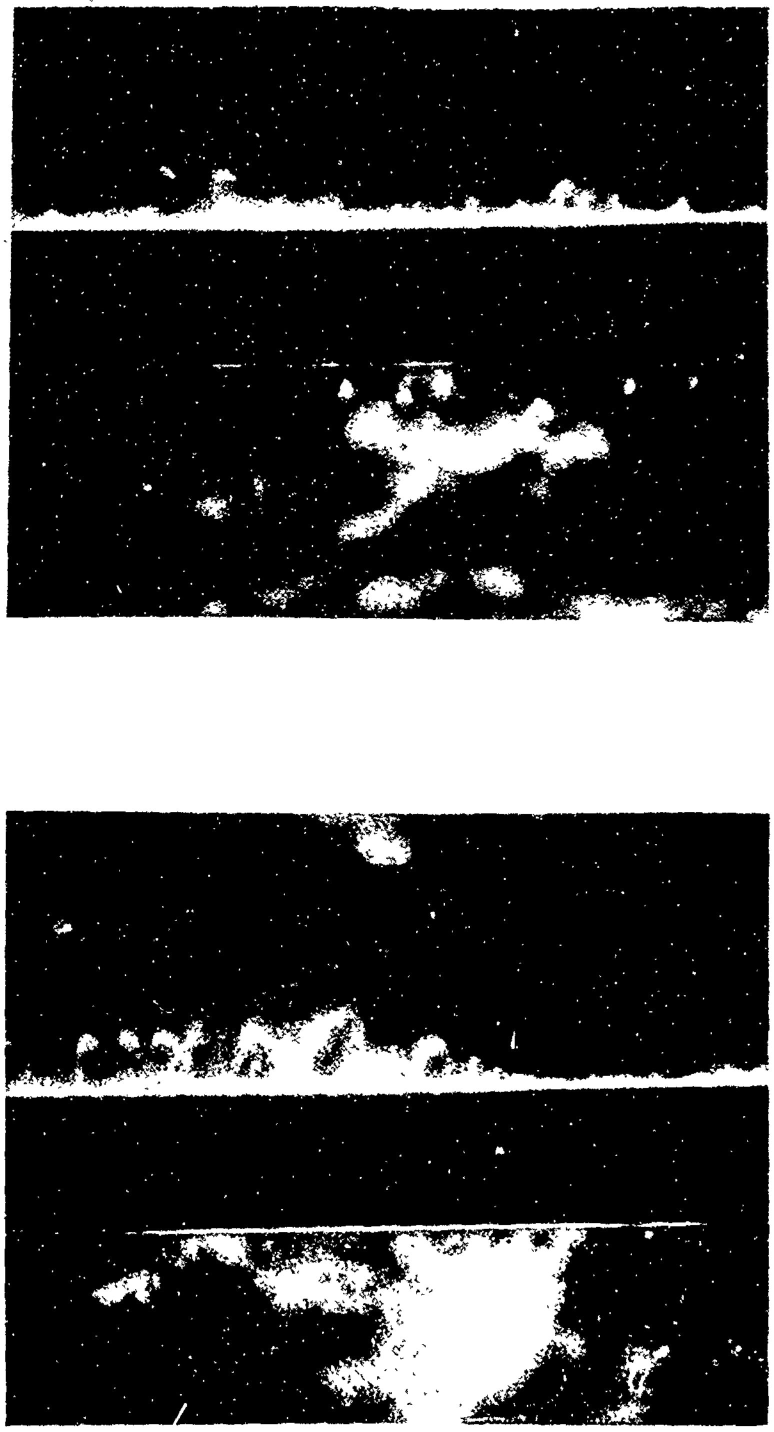

Figure 18

Schlieren Photographs at Position 4

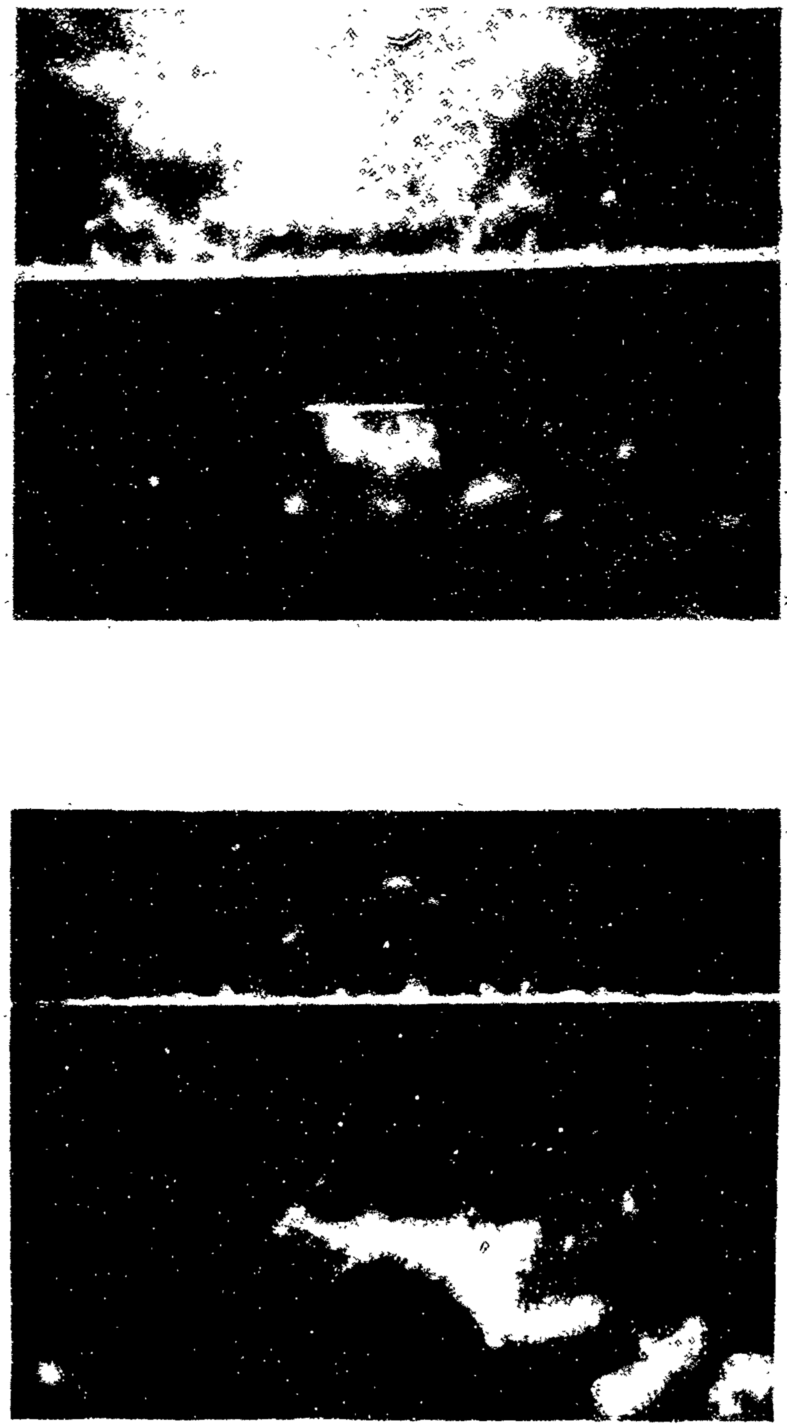

Figure 19

Schlieren Photographs at Position 5

VI. Conclusions and Recommendations

The results of this study of the free convective heat transfer from vibrating cylinders lead to the following conclusions:

1. There exist for each cylinder (1) a region at low vibration intensities in which vibration has no effect on the heat transfer rate; (2) a region at higher vibration intensities in which the variation in the heat transfer coefficient generally parallels the recommended forced convection curve of McAdams; and (3) a characteristic transition region in between.

2. In the region at higher vibration intensities where the heat transfer rate curve generally parallels the recommended forced convection curve of McAdams, there is an increased displacement from the McAdams curve with increased cylinder size for the range of cylinder sizes tested. For a given cylinder size, however, the heat transfer rate curve is independent of the temperature potential and dependent only on the vibration intensity within the range of temperature potentials used in this study.

3. In the transition region, the heat transfer rate is not solely a function of the vibration intensity. An increase in vibration frequency shifts the transition region in the direction of higher vibration intensities.

4. There is a considerable increase in turbulence in the boundary layer through the transition region which in turn justifies the marked increase in the heat transfer rate through this region.

5. The results of this study are in excellent agreement with the results of Neely for the 0.25 in diameter cylinder (Ref 3:30).

The following recommendations are made for future studies which might be undertaken:

1. That a qualitative study and analysis of the transition region phenomenon be conducted.

2. That the divergence of the variation of the heat transfer coefficient with vibration intensity from the recommended forced convection curve of McAdams be investigated.

Bibliography

1. Fand, R. M., and J. Kaye. "The Influence of Vertical Vibrations on Heat Transfer by Free Convection from a Horizontal Cylinder." International Developments in Heat Transfer, Part II: 490-8 (1961).

2. McAdams, W. H., Heat Transmission (Third Edition). New York, New York: McGraw-Hill Book Co., Inc., 1954.

3. Neely, D. F., Effect of Vibration on Heat Transfer from Cylinders in Free Convection. Thesis (unpublished). Dayton, Ohio: Air Force Institute of Technology, August 1964.

4. Shine, A. J., and F. C. Jarvis. Effect of Vibration on the Heat Transfer Rate from Cylinders in Free Convection. Paper (unpublished). Dayton, Ohio: Air Force Institute of Technology, 1963.

5. Watson, W. J. Effect of Vibration on Heat Transfer from Cylinders Vibrated Sinusoidally within a Vertical Plane in Free Convection. Thesis (unpublished). Dayton, Ohio: Air Force Institute of Technology, December 1965.

Part II

Table of Contents

List of Figures

List of Symbols

a	Amplitude of vibration - in
A_w	Surface area of cylinder - ft^2
D	Outside diameter of cylinder - ft^2
E	Voltage drop across cylinder - volts
f	Frequency of vibration - cps
g	Gravitational acceleration - 32.2 ft/sec^2
Gr	Grashof number, $D^3 \beta g(t_w - t_a)/\nu_f^2$ - dimensionless
h	Local coefficient of heat transfer - B/hr ft^2F
I	Current through cylinder - amps
k_f	Thermal conductivity of air at t_f - B/hr ft F
L	Length of cylinder between voltage measurements - ft
Nu	Nusselt number, hD/K_f - dimensionless
Pr	Prandtl numb - dimensionless
Q_c	Total convective heat loss - B/hr or watts
Q_r	Total radiation heat loss - B/hr or watts
Re	Vibration Reynolds number, $4afD/\nu_f$ - dimensionless
T_a	Temperature of ambient air - R
t_a	Temperature of ambient air - F
T_f	Temperature of boundary layer fluid, $(T_a + T_w)/2$ - R
t_f	Temperature of boundary layer fluid, $(t_a + t_w)/2$ - F
T_w	Temperature of cylinder wall - R
t_w	Temperature of cylinder wall - F

V	Volume of cylinder - ft^3
β	Coefficient of volumetric expansion, $1/T_f$ - R^{-1}
ϵ	Radiation emissivity of cylinder surface - dimensionless
ν	Kinematic viscosity of air at t_f - ft^2/sec
π	Constant - 3.1416...
σ	Stefan-Boltzmann constant - 0.173×10^{-8} B/hr ft^2 R^4

Appendix A

Apparatus and Experimental Procedures

Apparatus

Arrangement of the apparatus used in this study is shown photographically in Figures 1 through 4. These photographs should supplement most of the description which follows:

Test Cylinders

The test cylinders were lengths of stainless steel tubing of three different diameters. Specific data is listed below.

Diameter	Length	Wall Thickness	Surface
0.12 in	42.6 in	0.020 in	Polished
0.25 in	43.375 in	0.028 in	Polished
0.75 in	46.0 in	0.020 in	Polished

An iron-constantan thermocouple was attached to the internal wall surface of each cylinder at the test point, the point of maximum vibration amplitude, to provide instantaneous monitoring of the cylinder wall temperature. The cylinder ends were closed with press-fit styrofoam to reduce heat losses by convection within the cylinder.

Vibration Assembly and Housing

For the Watson assembly, the test cylinder was mounted horizontally and clamped rigidly at each end to a vertical post. An electromagnetic vibrator was positioned directly below the test cylinder and six inches from the left mounting clamp. An aluminum vibrator drive rod transmitted controllable frequency and amplitude outputs to the test cylinder, and to some degree constrained the cylinder to vibrate in the vertical plane. An adjustable but constant axial tension was applied to the cylinder at its right end to permit selected variation in the natural response frequency of the cylinder and to compensate for thermal expansion. The test cylinder, clamps, and support posts were mounted in a 48 x 12 x 30 in enclosure to provide protection from the random convective air currents in the laboratory. The enclosure was vented top and bottom to permit free convection around the cylinder. An iron-constantan thermocouple was mounted at cylinder level and six inches from the cylinder test point within the enclosure to sense the ambient air temperature (Ref 5:5).

For the improved apparatus, the test cylinder was mounted horizontally in a three inch long steel clamp at either end. Each clamp was pinned to a nine inch high clamp support which allowed rotation in the vertical plane and constrained cylinder vibration to the same plane. The clamp supports were bolted to a five foot long piece of

5 x 1-7/8 in inverted channel iron which inturn was bolted to the top of a 26 x 28 x 49 in cement pedestal in the M. E. Laboratory. The left clamp support was adjustable along the channel iron to accommodate different cylinder lengths. An adjustable but constant axial tension was applied to the test cylinder at the left mounting clamp. The electromagnetic vibrator was bolted to the right side of the cement pedestal. The steel vibrator drive ro was connected to a moment arm extension of the right mounting clamp. The channel iron, clamps and supports, and test cylinder were mounted in a 60 x 20 x 30 in enclosure with removable front and back panels. An iron-constantan thermocouple for measuring the ambient temperature, was mounted at cylinder level and nine inches from the cylinder test point.

Cylinder Heating Power

A 28 volt, 100 amp power source was available from the M. E. Laboratory DC rectifier. This source was connected to a high resistance load bank which permitted 6 to 8 amp incremental changes in current. A 5.8 ohm, 10 amp, and a 2.3 ohm, 4 amp slide resistor were connected in parallel with the load bank to provide fine power adjustments. Power leads connected to metal clamps at either end of the test cylinder placed the cylinder in series with the resistance and an ammeter. The voltage pick-off leads were connected to the power clamps for the 0.12 in and 0.25 in diameter cylinders and were soldered to the 0.75 in diameter cylinder immediately inside the mounting clamps. The location of these voltage leads determined the cylinder lengths L used in computing the cylinder surface area A_w. These lengths are listed below:

Diameter	Run Series	Length
0.12 in	A, B, C	40.0 in
0.25 in	D, E, F	41.8 in
0.25 in	G, H	34.6 in
0.75 in	I, J	37.125 in

Temperature Measurement

Two temperature recorders were used during this study. A Minneapolis Honeywell Brown Electronik Recorder with a 50F to 300F range and 12 channels was used for the A through H series of runs. A Bristol Dynamaster Recorder with a 0F to 200F range and 16 channels was used for the I and J series of runs. For each recorder the ambient air sensing thermocouple was connected to one channel to provide a temperature monitor for each minute of operation. The cylinder wall thermocouple was connected in series to each of the remaining channels to provide a temperature monitor every four to five seconds.

Vibration Control and Measurement

Vibration frequency was controlled through adjustment of an audio frequency oscillator contained in the vibrator power supply cabinet. Actual frequency measurements, however, were determined with a General Radio Company strobotac.

Vibration amplitude was controlled by a power rheostat in the vibrator power supply. In order to measure the amplitude, a photographic arrangement was used. The light from a mercury lamp unit was passed through a condensing lens onto a 1/32 in pin hole. The resulting point source of light was located at the focal length of a 7.5 in parabolic mirror which directed a parallel light beam through a vertical 1/32 in slit in the rear panel of the enclosure, across the vibrating cylinder, and through a glass window in the front panel. The shadow image of the vibrating cylinder was reflected by a second parabolic mirror onto a 2 in rotating flat mirror which swept the image across the aperture to a Polaroid camera containing type 47 film. The camera was mounted on the end of a plywood housing with an extendable bellows section which contained the aperture and a manually operated shutter. Knife scratches were inscribed on the photograph across the vibration peaks and the double amplitude was measured with a microscopic comparator. Figure 5 shows examples of the photographs used to determine vibration amplitude.

For the Schlieren photographs, the rotating mirror was replaced with a 4 in plane mirror and the 1/32 in slit was removed to provide a more lateral view of the cylinder. A knife edge was located between the 4 in plane mirror and the camera aperture. A five microsecond spark lamp was installed in place of the mercury lamp; the spark feature also served as the camera shutter.

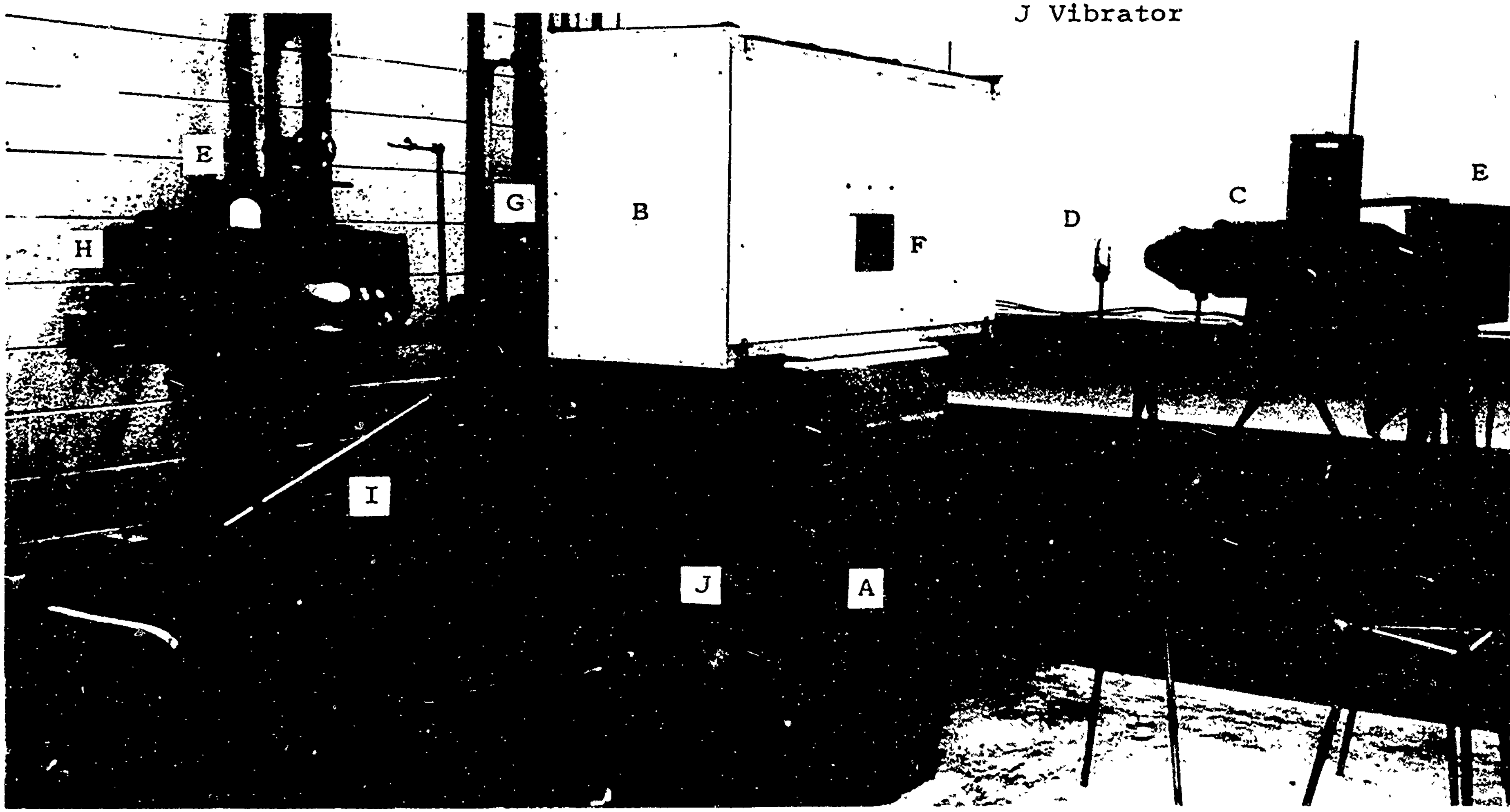

Figure 1
Photograph of General Arrangement of Test Apparatus

A Cement pedestal
B Enclosure
C Hooded light source
D Plane mirror
E Parabolic mirror
F 1/32 in slit
G Rotating plane mirror
H Polaroid camera
I Variac
J Vibrator

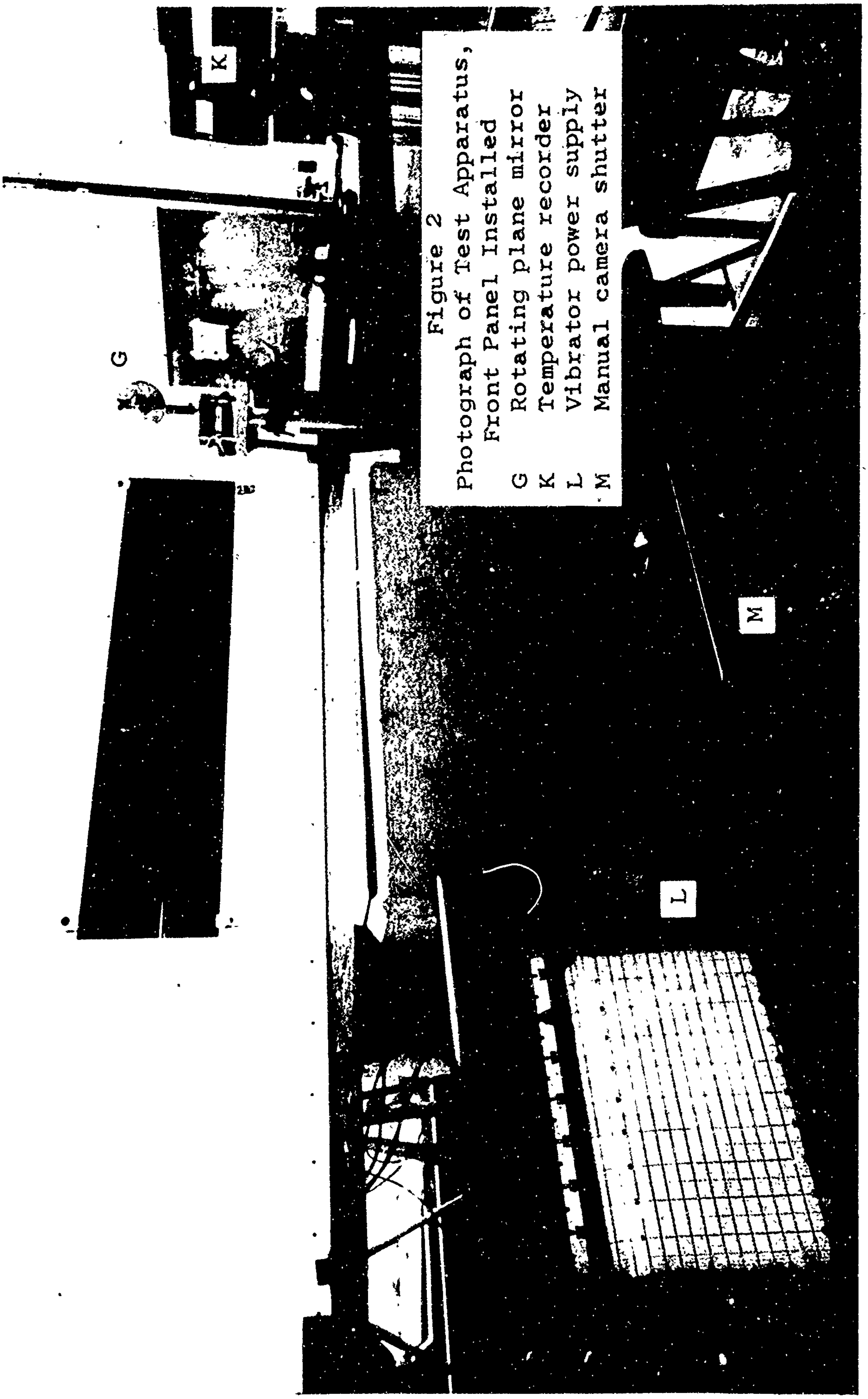

Figure 2
Photograph of Test Apparatus, Front Panel Installed

G Rotating plane mirror
K Temperature recorder
L Vibrator power supply
M Manual camera shutter

Figure 3

Photograph of Enclosure and Test Cylinder, Front Panel Removed

F 1/32 in slit
N Channel iron
O Vibrator drive rod
P Tension cable and pulley
Q Thermocouple (t_a)
R Thermocouple (t_w)
S DC Power lead
T DC Voltage lead

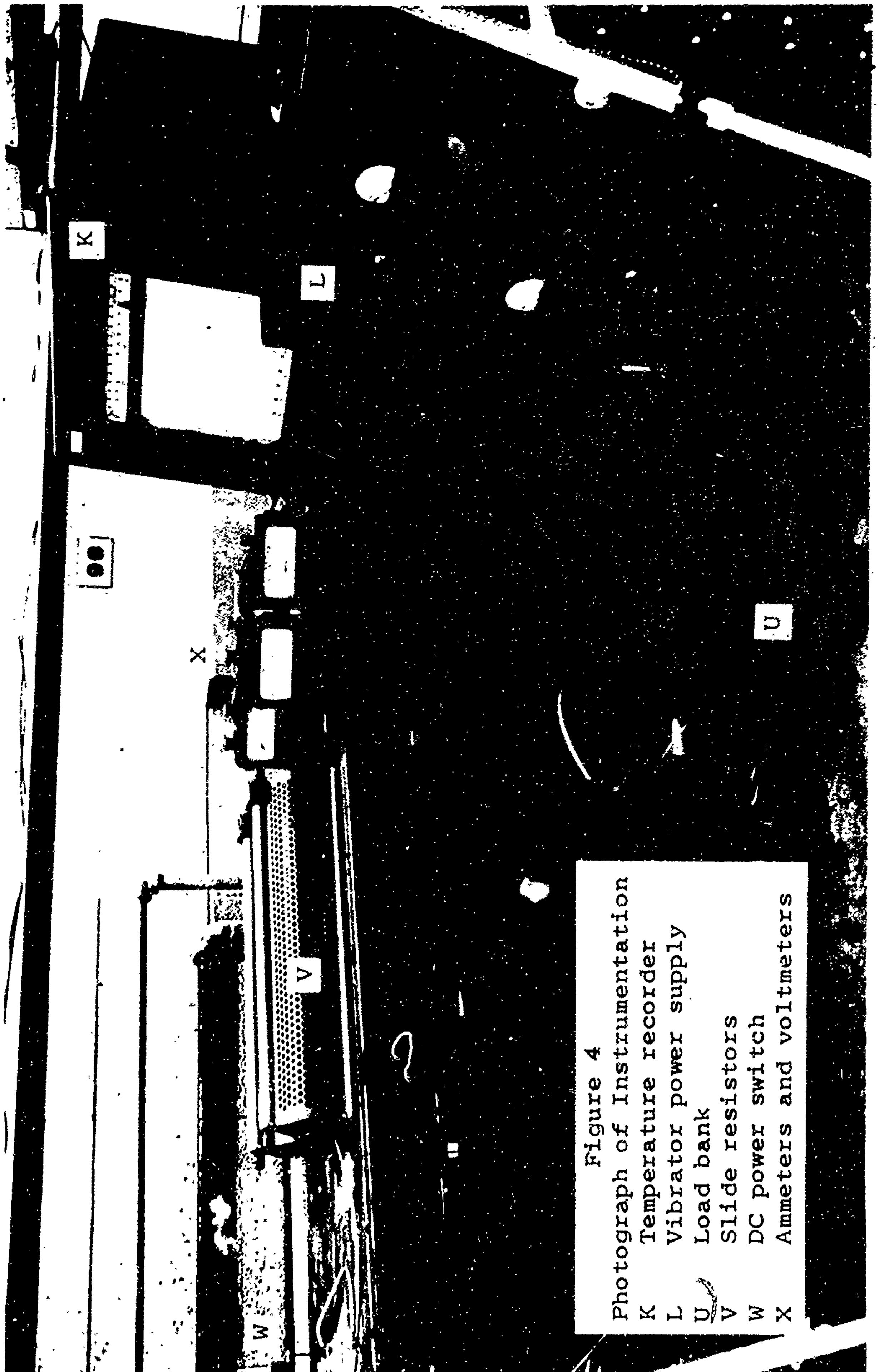

Figure 4
Photograph of Instrumentation
K Temperature recorder
L Vibrator power supply
U Load bank
V Slide resistors
W DC power switch
X Ammeters and voltmeters

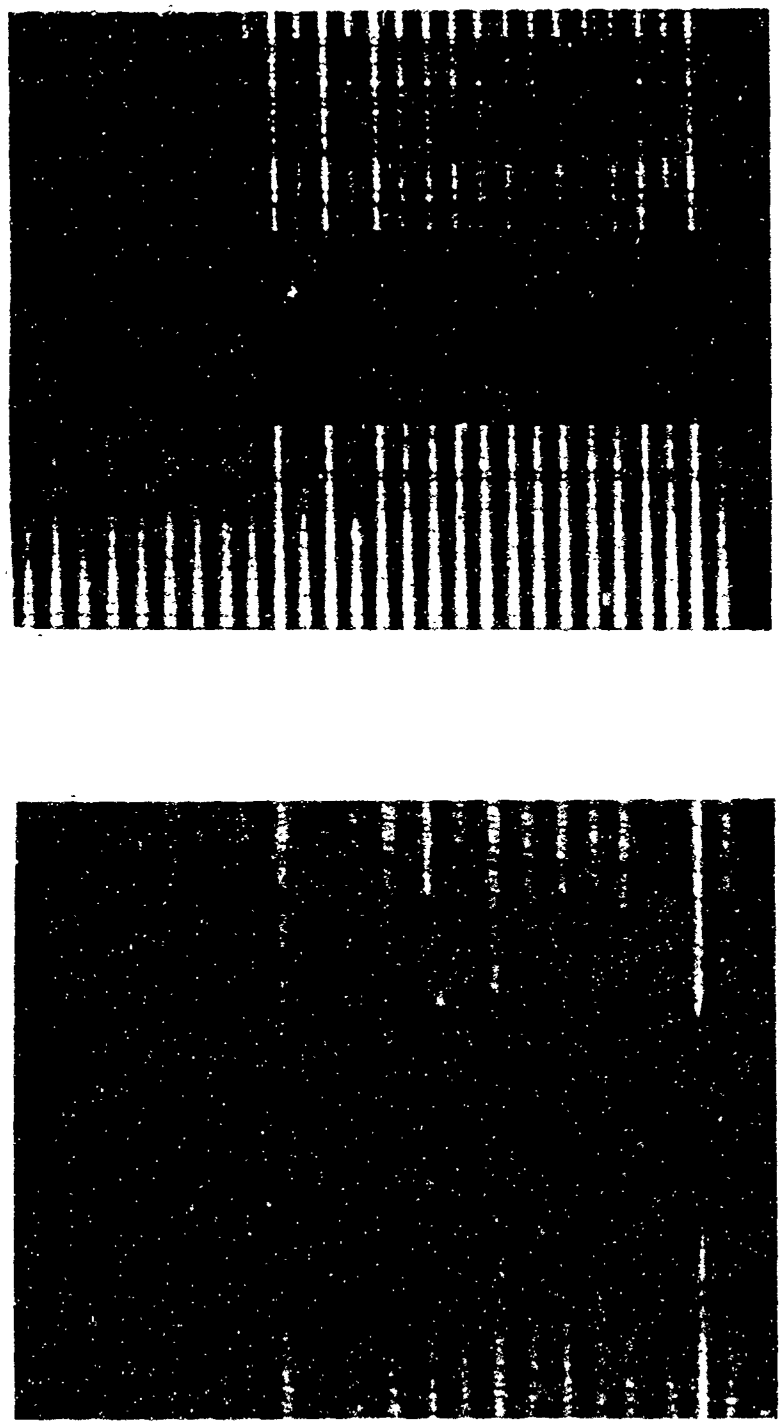

Figure 5

Photographs of Static and Vibrating
0.75 in Diameter Cylinder

Experimental Procedure

The static test cylinder was initially heated to a selected temperature potential. The current, voltage, ambient air temperature, and cylinder wall temperature were recorded. A photograph of the static cylinder was taken to provide a scale factor for computing subsequent vibration amplitudes. The photographic procedure consisted of the following: (1) the room lights were turned off; (2) the camera slide was removed; (3) as the image from the rotating mirror passed the camera aperture, the manually operated shutter was opened momentarily; (4) the camera slide was re-installed; and (5) the room lights turned back on. This procedure was also used for all photographs taken of the vibrating cylinder.

The vibrator was turned on and the frequency adjusted to the natural response frequency of the cylinder. The vibration amplitude was increased incrementally. The current, voltage, ambient air temperature, cylinder wall temperature, and frequency were recorded and a photograph was taken for each incremental increase in amplitude. This procedure was continued until a decrease in the temperature potential, which indicated an increase in heat transfer rate, was noted. From that point on, the current was increased incrementally and the vibration amplitude was adjusted until the selected temperature potential was again obtained and stabilized. The current voltage, ambient air temperature, cylinder wall temperature, and frequency were recorded, and a photograph taken for each incremental increase in current. This procedure was continued through each series of test runs.

Development of Equations

Equation for Calculating Nu

Development of the working equation for determining the local Nu at the test point on the cylinder involved the following assumptions:

a. The electrical power per unit volume delivered to the cylinder was constant between voltage pick-off points.

b. Axial heat conduction along the cylinder at the test point was negligble.

c. Radiation heat losses were a function of the temperature potential and not a function of vibration.

Axial temperature profiles were experimentally determined for the 0.25 in diameter cylinder at t_w-t_a = 100F and for the 0.75 in diameter cylinder at t_w-t_a = 50F and t_w-t_a = 100F by moving an iron-constantan thermocouple at measured intervals along the inner wall of the static cylinder. The resulting temperature profiles are shown in Figures 6, 7, and 8. Since the temperature gradients were essentially flat over a considerable portion of the cylinder including the center test point, the axial heat conduction was shown to be negligible. Similar results were arbitrarily assumed for the 0.12 in diameter cylinder.

The power per unit volume was experimentally determined over selected intervals of the static 0.75 in diameter cylinder at $t_w - t_a = 50F$. The initial interval was 8 in, 4 in either side of the center test point. The second interval was 10 in, 5 in either side of the center test point. Subsequent intervals were determined in the same manner across the length of the cylinder until the vibration test voltage pick-off points were reached. At each interval the voltage drop across the interval was determined using a Weston Analyzer with a 1.6 volt scale. The current was maintained constant. Volumes were computed assuming a constant cross sectional area and using the selected interval. Results are shown in Figure 4 and within the accuracy of measurements the power per unit volume was constant over each interval tested. Similar results were arbitarily assumed for the other cylinders and temperature potentials.

The basic equation for the local convective heat loss can be given by

$$\frac{Q_c dV}{V} = hdA(t_w - t_a)$$

This can be rewritten as

$$\frac{Q_c A_x dx}{V} = hcdx(t_w - t_a)$$

Where c = perimeter of the cylinder. Furthermore,

since $\frac{Ax}{V} = \frac{1}{L}$

$$\frac{Q_c}{L} = hc(t_w - t_a)$$

$$Q_c = hcL(t_w - t_a)$$

$$Q_c = hA_w(t_w - t_a)$$

$$h = \frac{Q_c}{A_w(t_w - t_a)}$$

$$Nu = \frac{Q_c \, D}{A_w k_f (t_w - t_a)}$$

Now $Q_c = EI - Q_r$ where EI, the power input, can be measured and Q_r must be determined independently. Hence, the local Nu can be determined using measurable quantities with the exception of Q_r.

The working equation with Q_c expressed in watts is

$$Nu = 3.413 \frac{Q_c D}{A_w k_f (t_w - t_a)} \qquad (1)$$

<u>Equation for Calculation of Q_r</u>

The basic equation for calculation of Q_r (B/hr) is given by

$$Q_r = \sigma \epsilon A_w (T_w^4 - T_a^4)$$

Evaluation of the emissivity was accomplished by forcing the static free convective heat transfer rate obtained by the apparatus of this study to agree with the recommended free convection curve of McAdams (Ref 2:176). Knowing Q_c in this case, Q_r could be determined by subtracting Q_c

from the measured EI; hence, the emissivity could be determined and assuming it to be constant in the temperature ranges tested, it could be reapplied to all data. Below is a summary of calculations made to determine the emissivity for each cylinder based on the recommended free convection curve of McAdams.

Cylinder	Run	GrPr	Nu	Q_r(watts)	ϵ
0.12 in OD	A-1	105	2.12	0	0.0
	B-1	143	2.16	2.3	0.22
0.25 in OD	D-1	919	3.07	1.22	0.139
	E-1	1226	3.22	3.2	0.138
	G-1	824	2.96	0.94	0.138
0.75 in OD	I-1	15850	5.63	0.16	0.015
	J-1	25000	6.03	1.44	0.059

The following emissivities were selected based on the above data:

Cylinder	ϵ
0.12 in OD	0.10
0.25 in OD	0.14
0.75 in OD	0.05

The chosen emissivities were used to calculate the test Nu in all data taken. Below is summarized the deviation in the free convective Nu as compared to McAdams:

Cylinder	Run	Nu(test)	Nu(McAdams)	Error %
0.12 in OD	A-1	1.91	2.12	5.2
	B-1	2.27	2.16	5.1
0.25 in OD	D-1	3.10	3.07	1.0
	E-1	3.20	3.22	0.6
	G-1	2.96	2.96	0.0
0.75 in OD	I-1	5.46	5.63	3.0
	J-1	6.07	6.03	1.0

The working equation for determining Q_r in watts is

$$Q_r = \frac{17.57}{60}(0.173)\ A_w \epsilon \left[\left(\frac{T_w}{100}\right)^4 - \left(\frac{T_a}{100}\right)^4\right] \qquad (2)$$

where ϵ is one of the selected values above depending on the cylinder as identified by the diameter.

Equation for Calculating Re

The average vibrational velocity, 4af, was used in calculating Re. The working equation is

$$Re = \frac{4afD}{12\,\nu_f} = \frac{2afD}{6\,\nu_f} \qquad (3)$$

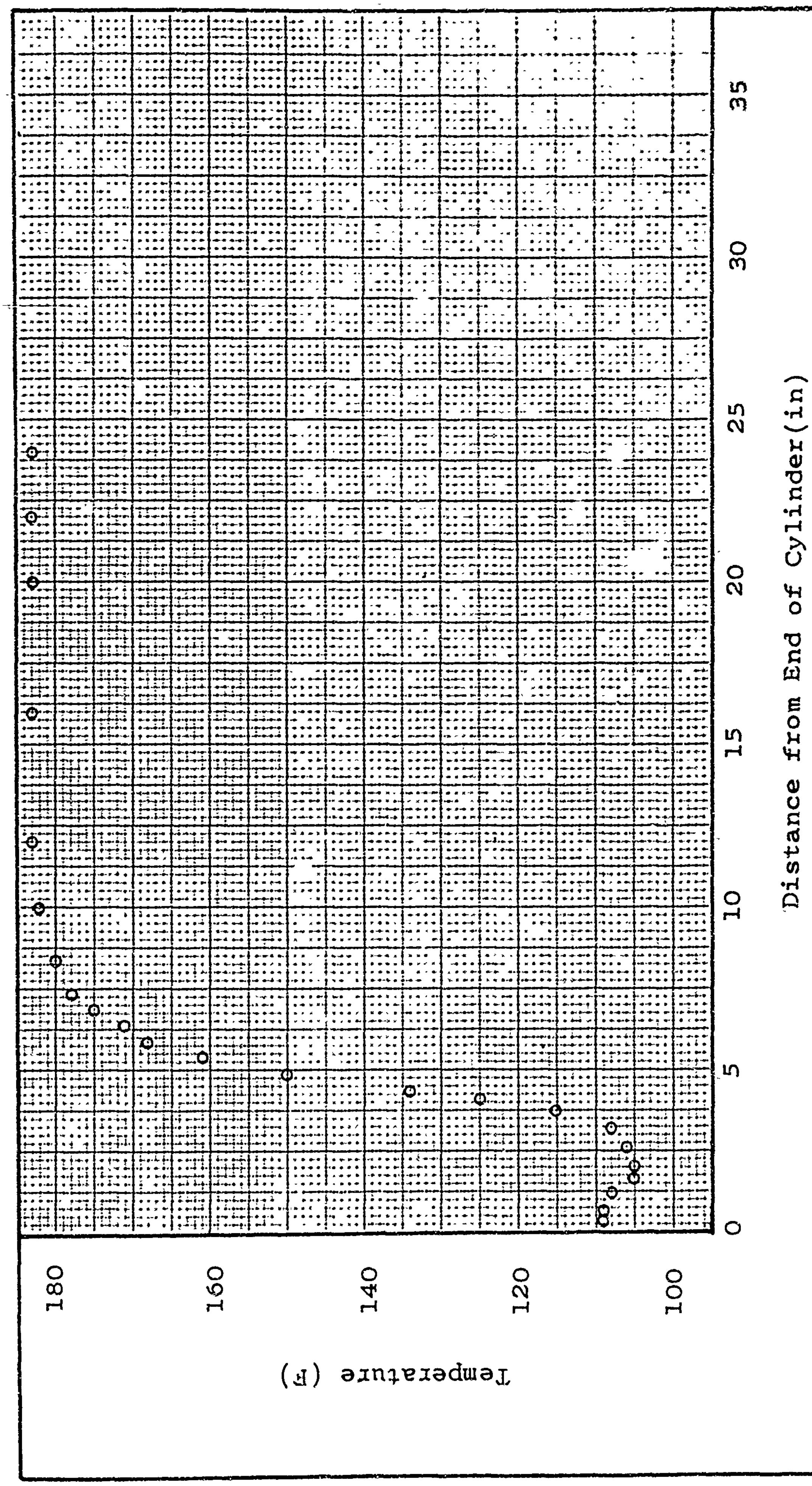

Figure 6

Temperature Profile in 0.25 in Diameter Cylinder with $(t_w - t_a) = 93$ F

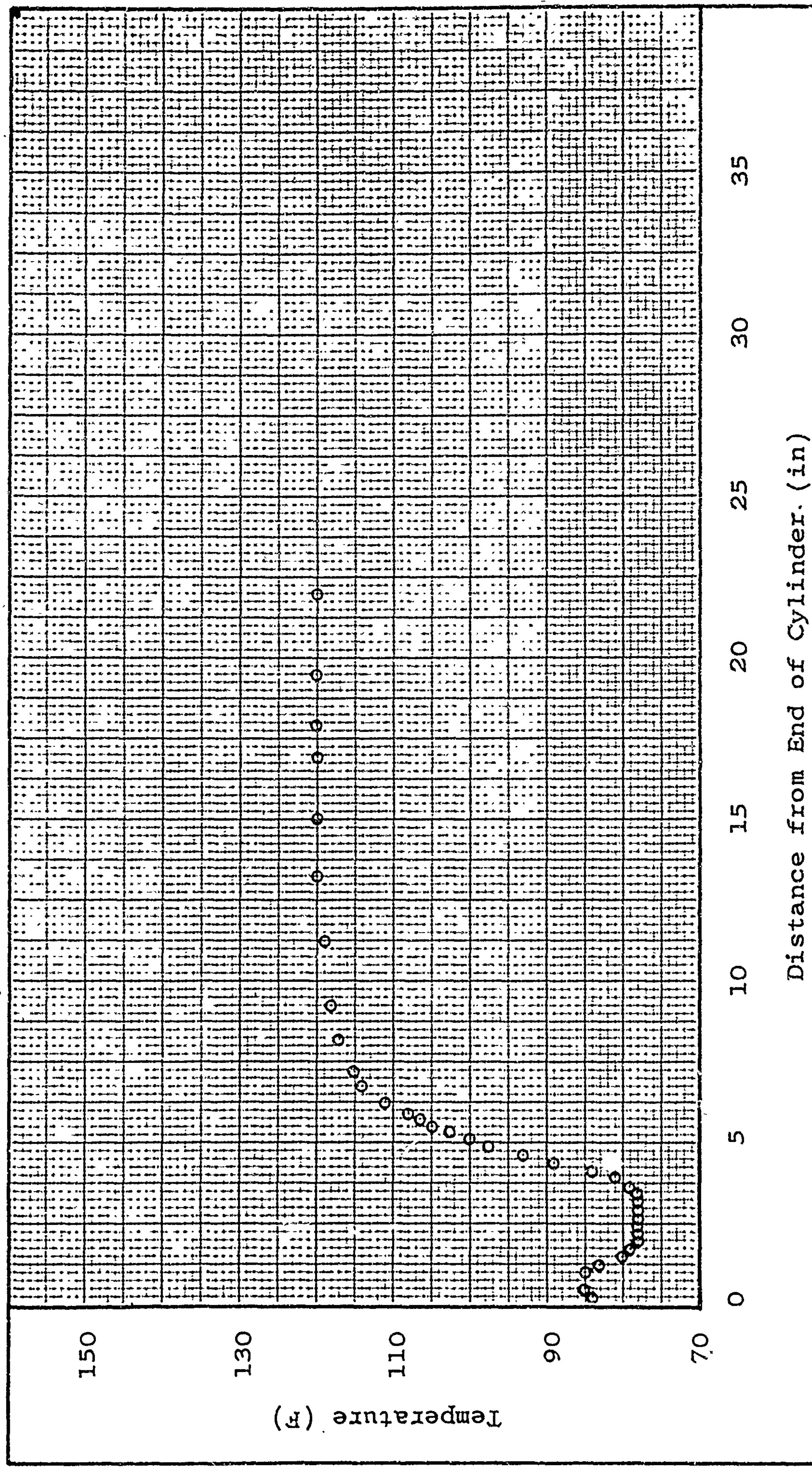

Figure 7

Temperature Profile in 0.75 in Diameter Cylinder with $(t_w - t_a) = 50$ F

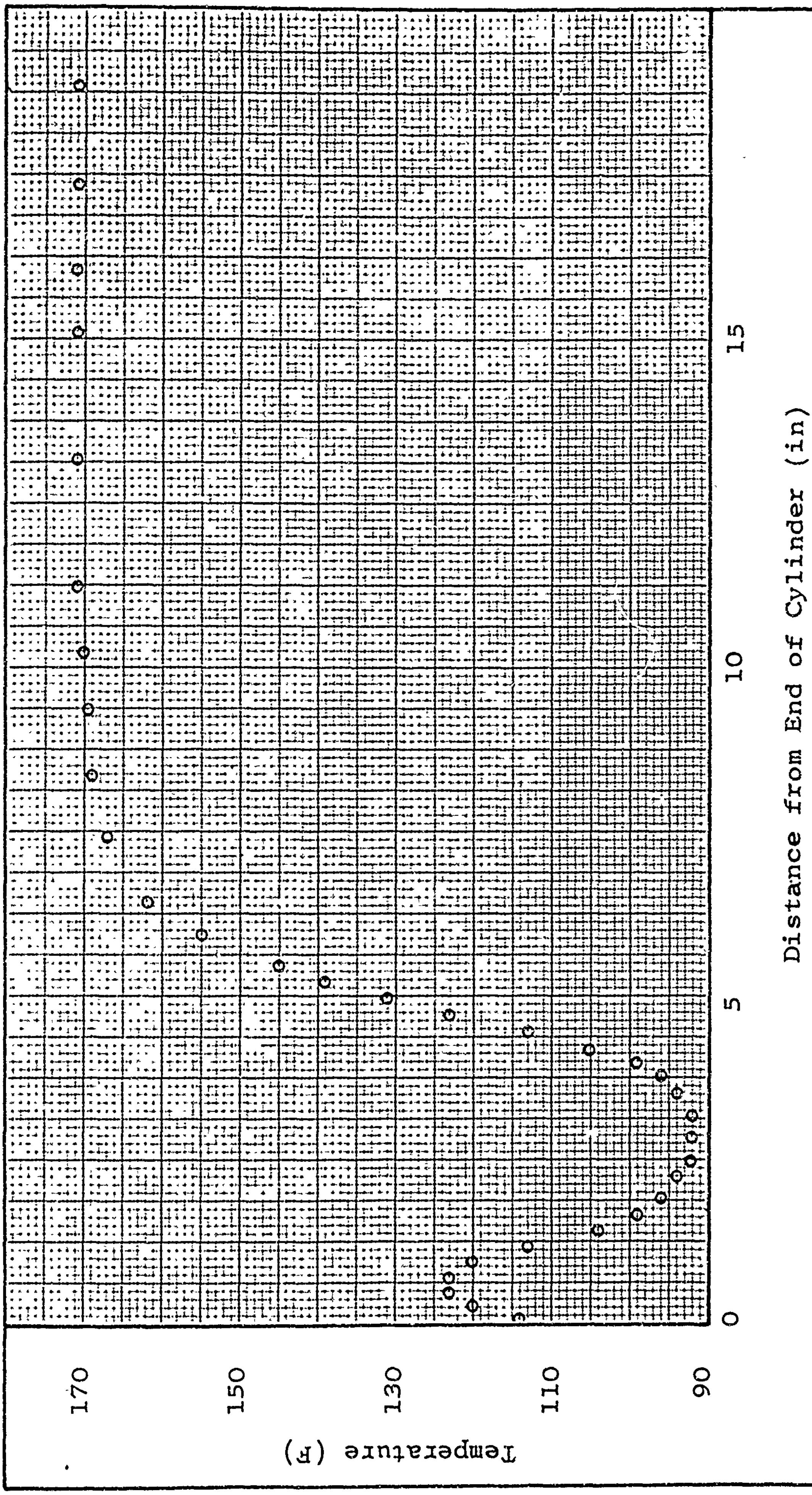

Figure 8

Temperature Profile in 0.75 in Diameter Cylinder with $(t_w - t_a) = 100$ F

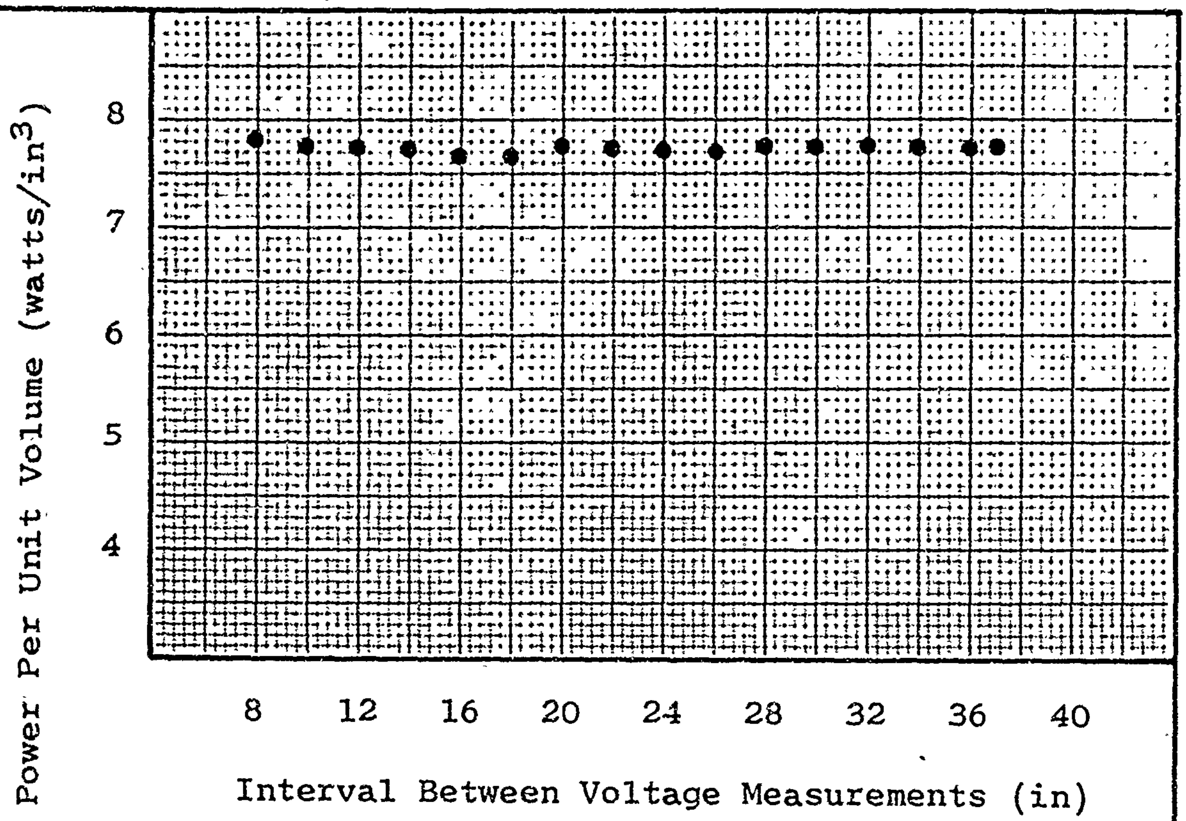

Figure 9

Power Per Unit Volume Across Static 0.75 in Diameter Cylinder with t_w-t_a = 50F

Error Analysis

Electrical Measurements

Measurements of the voltage E and current I were used to calculate the total power input to the cylinder. The voltmeters and ammeters were calibrated by the Electrical Engineering Department against a meter standard accurate to $\frac{1}{4}$ of 1%. Instrument reading errors were judged to be $\pm$ 10% of the smallest scale reading. Accuracy data for the meters used is presented in Table C-1.

Frequency Measurement

The vibration frequency was measured with a strobotac calibrated prior to each series of runs. The accuracy of the instrument when calibrated was $\pm$ 1% of the high scale. This amounted to a possible error of $\pm$ 0.617 cps.

Amplitude Measurement

The double amplitude of vibration was measured with a micro comparator between knife scratches scribed across the amplitude peaks on the Polariod film. The comparator could be read to the fourth decimal place. The primary

Table C-1

Electrical Measurement Data Errors

Instrument	Scale	Smallest Scale Graduation	Closest Approximation	Maximum Instrument Error	Maximum Total Error in Data
Ammeter	50 amps	1.50 amps	$\pm$ 0.05 amps	$\pm$ 0.125 amps	$\pm$ 0.175 amps
Ammeter	150 amps	1.00 amps	$\pm$ 0.1 amps	$\pm$ 0.375 amps	$\pm$ 0.475 amps
Voltmeter	15 volts	0.10 volts	$\pm$ 0.01 volts	$\pm$ 0.0375 volts	$\pm$ 0.0475 volts
Voltmeter	3 volts	0.02 volts	$\pm$ 0.002 volts	$\pm$ 0.0075 volts	$\pm$ 0.0095 volts

source of error was the scribing of the double amplitude. This error was estimated to be ± 0.001 in. In addition, the scale factor had an estimated ± 0.001 in error. The maximum total error in measuring the double amplitude was ± 0.002 in.

Temperature Measurement

The Brown Recorder, used in the A through H series of runs, was calibrated over its 50F to 300F range by personnel in the Aerospace Research Laboratories. The entire temperature measuring system, recorder and iron-constantan thermocouples, was re-checked at ambient air and boiling water temperatures against a mercury in glass thermometer. Agreement was within the ability to read the scales. The Bristol Dynamaster Recorder, used in the I and J series of runs, was calibrated over its 0F to 200F range with an accurate Leeds and Northrup millivolt potentiometer. Since for either recorder the manufacturer could not guarantee an accuracy of better than ± 0.03 millivolts in the mechanical slide linkage, a possible error of ± 1F was assumed.

Overall Error

The maximum possible error in Nu is given by

$$\Delta Nu = \frac{3.413D}{A_w k_f}\left[\frac{E\Delta I}{(t_w-t_a)} + \frac{I\Delta E}{(t_w-t_a)} + \frac{EI\,\Delta(t_w-t_a)}{(t_w-t_a)^2}\right] \qquad (4)$$

The maximum possible error in Re is given by

$$\Delta Re = \frac{4D}{12\,\nu_f}(a\Delta f + f\Delta a) \qquad (5)$$

The largest overall error in Nu occurred for Run A-1 and was computed to be 7.1%. As the value of the Nu increased its relative error decreased.

The largest overall error in Re occurred for Run A-7 which also had the lowest Re (=8). It computed to 37½%. This resulted as a consequence of the relative values of the small measured amplitude of vibration and the estimated error involved in this measurement. The error in Re, however, dimenished rapidly as Re was increased and the general range of the Re errors was 2% to 5%.

Sample Calculations

The following calculations are based on Run I-34 for the 0.75 in diameter cylinder. The cylinder dimensions are:

$$D = 0.0626 \text{ ft} \qquad L = 3.09 \text{ ft}$$

The recorded test data are:

t_a = 87F I = 49.0 amps 2a = 0.6430 in

t_w = 137F E = 1.26 volts f = 43.2 cps

The following computations were performed:

$$t_f = \frac{t_w + t_a}{2} = \frac{137 + 87}{2} = 112\text{F}$$

$$t_w - t_a = 137 - 87 = 50\text{F}$$

$$EI = (1.26)(49.0) = 61.74 \text{ watts}$$

$$A_w = \pi DL = (3.1416)(0.0626)(3.09) = 0.609 \text{ ft}^2$$

The fluid properties at t_f = 112F were determined to be (Ref 1:504):

$$\nu_f = 18.83 \text{x} 10^{-5} \text{ ft}^2/\text{sec}$$

$$k_f = 0.01594 \text{ B/hr ft. F}$$

$$Pr = 0.704$$

The radiation heat loss was computed from Equation (1):

$$Q_r = \frac{17.57}{60}(0.173)A_w \epsilon \left[\left(\frac{T_w}{100}\right)^4 - \left(\frac{T_a}{100}\right)^4 \right]$$

where the emissivity ϵ = 0.05 (from Appendix B) and Q_r is given in watts.

$$Q_r = \frac{17.57}{60}(0.173)(0.609)(0.05)\left[\left(\frac{460 + 137}{100}\right)^4 - \left(\frac{460 + 87}{100}\right)^4\right]$$

$$Q_r = 0.58 \text{ watts}$$

Hence, the convective heat loss is

$$Q_c = EI - Q_r = 61.74 - 0.58 = 61.16 \text{ watts}$$

The Nusselt number from Equation (2) is

$$Nu = 3.413 \frac{Q_c D}{A_w k_f (t_w - t_a)}$$

$$Nu = 3.413 \frac{(61.16)(0.0626)}{(0.609)(0.01594)(50)}$$

$$Nu = 26.90$$

$$\frac{Nu}{Pr^{.3}} = \frac{26.90}{0.90} = 29.90$$

$$\text{Log } \frac{Nu}{Pr^{.3}} = 1.476$$

The Reynolds number from Equation (3) is

$$Re = \frac{4afD}{12\nu_f} = \frac{2afD}{6\nu_f}$$

$$Re = \frac{(0.6430)(43.2)(0.0626)}{6(18.83 \times 10^{-5})}$$

$$Re = 1539$$

$$\text{Log } Re = 3.187$$

The overall error in the Nusselt number from Equation (4) is

$$\Delta Nu = \frac{3.413D}{A_w k_f}\left[\frac{E\Delta I}{(t_w-t_a)} + \frac{I\Delta E}{(t_w-t_a)} + \frac{EI\Delta(t_w-t_a)}{(t_w-t_a)^2}\right]$$

ΔI = 0.475 amps ΔE = 0.0095 volts $\Delta(t_w-t_a)$ = 1F

$$\Delta Nu = \frac{(3.413)(0.0626)}{(0.609)(0.01594)}\left[\frac{(1.26)(0.475)}{50} + \frac{(49.0)(0.0095)}{50} + \frac{(61.74)(1)}{2500}\right]$$

$$\Delta Nu = 1.01$$

Error in Nu = 3.76%

The overall error in the Reynolds number from Equation (5) is

$$\Delta Re = \frac{4D}{12\nu_f}(a\Delta f + f\Delta a)$$

Δf = 0.617 cps Δa = 0.001 in

$$\Delta Re = \frac{4(0.0626)}{(12)(18.83\text{x}10^{-5})}\left[(0.3215)(0.617) + (43.2)(0.001)\right]$$

$$\Delta Re = 24.4$$

Error in Re = 1.59%

Table 1

Experimental Data for 0.12 in Diameter Cylinder

Run	f cps	2a in	t_w F	t_a F	$t_w - t_a$ F	I Amps	E Volts	EI Watts	Qr Watts	Qc Watts	$\frac{Nu}{Pr^{.3}}$	Log $\frac{Nu}{Pr^{.3}}$	Re	Log Re
A-1	0.0	0.0	168	68	100	5.80	1.70	9.86	0.39	9.47	2.13	0.328	0	--
A-2	27.3	0.0885	171	69	102	5.90	1.70	10.03	0.41	9.62	2.12	0.326	21	1.314
A-3	27.3	0.4220	170	70	100	9.10	2.70	24.55	0.39	24.16	5.42	0.734	99	1.997
A-4	27.3	0.6520	171	70	101	10.20	3.10	31.60	0.40	31.20	6.93	0.841	150	2.177
A-5	25.0	0.0370	167	67	100	5.85	1.70	9.95	0.39	9.56	2.15	0.332	8	0.906
A-6	25.0	0.0673	169	68	101	5.85	1.70	9.95	0.40	9.55	2.13	0.328	15	1.163
A-7	25.0	0.1300	170	69	101	5.90	1.70	10.03	0.40	9.52	2.12	0.326	38	1.449
A-8	24.3	0.4580	170	68	102	9.00	2.70	24.30	0.40	24.10	5.31	0.725	96	1.984
A-9	24.3	0.6830	170	69	101	10.00	3.00	30.00	0.40	29.60	6.48	0.812	143	2.157
A-10	33.5	0.1740	173	73	100	6.00	1.75	10.50	0.40	10.10	2.36	0.373	50	1.697
A-11	32.7	0.3480	173	73	100	8.50	2.50	21.25	0.40	20.85	4.67	0.669	97	1.988
A-12	32.7	0.5150	172	73	99	10.00	3.00	30.00	0.39	29.61	6.69	0.825	144	2.158
A-13	32.0	0.6820	175	74	101	11.25	3.45	38.80	0.41	38.39	8.48	0.928	185	2.268
A-14	41.7	0.1593	172	73	99	6.10	1.75	10.67	0.39	10.28	2.32	0.365	57	1.755
A-15	40.4	0.3475	172	73	99	9.25	2.80	25.90	0.39	25.51	5.67	0.760	120	2.079
A-16	27.1	0.2145	173	73	100	6.25	1.80	11.25	0.40	10.85	2.43	0.386	50	1.696
A-17	24.2	0.3470	174	73	101	7.75	2.25	17.43	0.41	17.02	3.77	0.576	72	1.856
A-18	33.4	0.2265	174	75	99	6.75	1.95	13.17	0.40	12.77	2.87	0.458	64	1.809
A-19	41.1	0.2295	174	75	99	7.25	2.10	15.22	0.40	14.82	3.34	0.524	80	1.905
A-20	40.6	0.7625	174	77	97	12.10	3.70	44.80	0.39	4[illegible].41	10.20	1.008	263	2.420
A-21	25.8	1.529	176	78	98	12.50	3.80	47.50	0.40	47.10	10.70	1.029	332	2.522
B-1	26.5	0.1255	274	73	201	9.10	2.80	25.48	1.04	24.44	2.54	0.405	25	1.390
B-2	26.5	0.1880	275	73	202	9.25	2.85	26.35	1.05	25.30	2.61	0.417	37	1.565

Table I (Cont'd)

Experimental Data for 0.12 in Diameter Cylinder

Run	f cps	2a in	t_w F	t_a F	t_w-t_a F	I Amps	E Volts	EI Watts	Qr Watts	Qc Watts	$\frac{Nu}{Pr^{.3}}$	Log $\frac{Nu}{Pr^{.3}}$	Re	Log Re
B-3	26.5	0.2365	272	74	198	9.40	2.90	27.25	1.02	26.23	2.77	0.442	46	1.667
B-4	25.2	0.5760	273	75	198	13.50	4.30	58.05	1.03	57.02	6.00	0.778	107	2.029
B-5	25.3	0.6660	273	76	197	14.00	4.45	62.30	1.03	61.27	6.48	0.812	124	2.093
B-6	25.3	0.7800	274	76	198	14.50	4.60	66.70	1.03	65.67	6.90	0.839	145	2.161
B-7	25.3	0.9750	278	76	202	15.00	4.80	72.00	1.07	70.93	7.28	0.862	180	2.256
B-8	25.3	1.104	277	76	201	15.50	5.00	77.50	1.06	76.44	7.89	0.897	204	2.310
B-9	25.3	1.305	276	76	200	16.00	5.15	82.45	1.05	81.40	8.46	0.927	242	2.384
B-10	26.3	0.2645	276	75	201	10.00	3.10	31.00	1.05	29.95	3.10	0.491	51	1.708
B-11	26.3	0.3570	278	75	203	11.40	3.60	41.10	1.07	40.03	4.12	0.615	69	1.837
B-12	26.1	0.4580	274	75	199	12.50	3.95	49.40	1.04	48.36	5.06	0.704	88	1.944
C-1	26.8	0.1365	175	74	101	6.00	1.70	10.20	0.40	9.80	2.16	0.334	32	1.498
C-2	27.3	0.0966	176	75	101	6.00	1.70	10.20	0.41	9.79	2.15	0.332	22	1.349
C-3	26.7	0.2285	175	75	100	6.50	1.85	12.02	0.40	11.62	2.59	0.413	52	1.714
C-4	26.8	0.2540	176	75	101	7.00	2.00	14.00	0.41	13.59	3.00	0.477	58	1.762
C-5	27.0	0.3110	176	75	101	7.50	2.20	16.50	0.41	16.09	3.55	0.551	71	1.852
C-6	26.3	0.3490	176	75	101	8.00	2.35	18.80	0.41	18.39	4.05	0.607	78	1.891
C-7	26.8	0.3820	176	76	100	8.50	2.50	21.25	0.40	20.85	4.64	0.667	87	1.938
C-8	26.4	0.4360	176	76	100	9.00	2.70	24.30	0.40	23.90	5.22	0.726	98	1.989
C-9	26.2	0.5400	175	76	99	9.50	2.85	27.05	0.40	26.65	5.99	0.777	120	2.079
C-10	26.0	0.6100	176	76	100	10.00	3.00	30.00	0.40	29.60	6.58	0.818	134	2.128
C-11	41.8	0.1182	176	76	100	6.00	1.70	10.20	0.40	9.80	2.18	0.338	42	1.622
C-12	41.8	0.1028	176	76	100	6.00	1.70	10.20	0.40	9.80	2.18	0.338	36	1.561
C-13	41.5	0.1816	176	76	100	6.50	1.85	12.02	0.40	11.62	2.59	0.413	64	1.805

Table I (Cont'd)

Experimental Data for 0.12 in Diameter Cylinder

Run	f cps	2a in	t_w F	t_a F	$t_w - t_a$ F	I Amps	E Volts	EI Watts	Qr Watts	Qc Watts	$\frac{Nu}{Pr^{.3}}$	Log $\frac{Nu}{Pr^{.3}}$	Re	Log Re
C-14	40.75	0.2085	175	76	99	7.00	2.00	14.00	0.40	13.60	3.06	0.486	72	1.858
C-15	41.25	0.2700	175	76	99	8.00	2.35	18.80	0.40	18.40	4.13	0.616	94	1.975
C-16	41.25	0.3050	176	76	100	8.50	2.50	21.25	0.40	20.85	4.64	0.667	106	2.027
C-17	4' 1	0.3225	176	77	99	9.00	2.70	24.30	0.40	23.90	5.37	0.730	112	2.049
C-18	40.75	0.3400	176	77	99	9.50	2.85	27.05	0.40	26.65	5.99	0.777	117	2.068
C-19	40.75	0.3950	176	76	100	10.00	3.00	30.00	0.40	29.60	6.58	0.818	136	2.134

Table II

Experimental Data for 0.25 in Diameter Cylinder

Run	f cps	2a in	t_w F	t_a F	$t_w - t_a$ F	I Amps	E Volts	EI Watts	Q_r Watts	Q_c Watts	$\frac{Nu}{Pr^{.3}}$	Log $\frac{Nu}{Pr^{.3}}$	Re	Log Re
D-1	0.0	0.0	175	75	100	16.5	1.05	17.32	1.23	16.09	3.45	0.538	0	--
D-2	50.0	0.1445	176	76	100	16.5	1.05	17.32	1.24	16.08	3.44	0.537	127	2.104
D-3	50.0	0.1743	177	76	101	16.5	1.05	17.32	1.26	16.06	3.41	0.533	152	2.182
D-4	50.2	0.1760	175	77	98	17.0	1.10	18.60	1.21	17.39	3.79	0.579	156	2.192
D-5	50.3	0.1901	178	78	100	18.0	1.15	20.70	1.26	19.44	4.15	0.618	167	2.224
D-6	50.4	0.2175	178	78	100	19.0	1.20	22.80	1.26	21.54	4.59	0.662	192	2.283
D-7	49.2	0.2305	178	79	99	20.0	1.30	26.00	1.24	24.76	5.32	0.726	198	2.297
D-8	48.8	0.2455	178	79	99	21.0	1.35	28.35	1.24	27.11	5.83	0.766	209	2.320
D-9	48.6	0.2740	178	79	99	23.0	1.50	34.50	1.24	33.26	7.15	0.854	233	2.367
D-10	48.1	0.3280	179	80	99	27.0	1.75	47.25	1.25	46.00	9.79	0.991	275	2.423
D-11	48.1	0.3740	181	81	100	29.0	1.90	55.10	1.27	53.83	11.42	1.058	322	2.508
D-12	48.4	0.238	176	76	100	25.0	1.60	40.00	1.24	38.76	8.29	0.919	242	2.384
D-13	48.8	0.4840	179	79	100	31.0	2.05	63.50	1.26	62.24	13.25	1.122	412	2.615
E-1	49.4	0.0535	277	76	201	24.5	1.60	39.20	3.25	35.95	3.57	0.553	40	1.605
E-2	50.0	0.1094	278	76	202	24.5	1.60	39.20	3.28	35.92	3.55	0.550	83	1.920
E-3	50.0	0.1485	278	76	202	24.5	1.60	39.20	3.28	35.92	3.55	0.550	113	2.053
E-4	50.0	0.1808	277	76	201	25.0	1.65	41.25	3.25	38.00	3.77	0.576	138	2.137
E-5	48.2	0.2425	277	75	202	27.0	1.80	48.60	3.28	45.32	4.47	0.650	178	2.252
E-6	48.25	0.2710	277	76	201	29.0	1.95	56.60	3.25	53.35	5.28	0.723	199	2.300
E-7	48.4	0.2880	276	76	200	31.0	2.10	65.10	3.22	61.88	6.18	0.791	212	2.327
E-8	48.5	0.3000	278	76	202	33.0	2.30	76.00	3.28	72.72	7.17	0.856	222	2.345
E-9	45.8	0.3575	278	77	201	35.0	2.45	85.80	3.28	82.52	8.16	0.912	248	2.394
E-10	46.3	0.3780	277	77	200	37.0	2.60	96.25	3.25	93.00	9.26	0.967	266	2.425

Table II (Cont'd)

Experimental Data for 0.25 in Diameter Cylinder

Run	f cps	2a in	t_w F	t_a F	t_w-t_a F	I Amps	E Volts	EI Watts	Q_r Watts	Q_c Watts	$\frac{Nu}{Pr^{.3}}$	Log $\frac{Nu}{Pr^{.3}}$	Re	Log Re
E-11	45.5	0.4505	278	78	200	39.0	2.75	107.2	3.28	103.9	10.32	1.014	311	2.493
E-12	44.7	0.5280	279	78	201	41.0	2.95	121.0	3.28	117.7	11.63	1.066	358	2.554
E-13	43.65	0.5990	279	79	200	43.0	3.10	133.3	3.28	130.0	12.91	1.111	396	2.598
F-1	46.75	0.3830	128	78	50	20.0	1.30	26.00	0.55	25.45	11.27	1.052	340	2.531
F-2	46.8	0.4120	128	78	50	21.0	1.33	27.90	0.55	26.95	11.91	1.076	366	2.563
F-3	45.8	0.5180	129	79	50	22.0	1.40	30.80	0.55	30.25	13.39	1.127	449	2.652
G-1	0.0	0.0	172	80	92	15.5	0.82	12.71	0.95	11.76	3.29	0.517	0	--
G-2	19.3	0.2870	172	80	92	15.5	0.82	12.71	0.95	11.76	3.29	0.517	98	1.989
G-3	18.0	0.2280	173	81	92	15.5	0.82	12.71	1.00	11.71	3.28	0.516	72	1.858
G-4	19.9	0.2210	171	78	93	15.5	0.82	12.71	1.00	11.71	3.26	0.513	78	1.892
G-5	20.0	0.2220	172	79	93	15.5	0.82	12.71	1.00	11.71	3.26	0.513	78	1.892
G-6	19.2	0.3680	170	80	90	18.0	0.98	17.63	0.97	16.66	4.77	0.679	125	2.097
G-7	19.0	0.4370	173	81	92	21.0	1.14	23.95	1.00	22.95	6.43	0.808	146	2.164
G-8	19.25	0.5810	175	82	93	24.0	1.33	31.92	1.02	30.90	8.52	0.930	196	2.292
G-9	18.9	0.8850	176	83	93	27.0	1.49	40.25	1.02	39.23	10.81	1.034	292	2.465
G-10	19.85	0.340	176	82	94	17.0	0.91	15.47	1.03	14.44	3.94	0.596	118	2.072
G-11	19.9	0.3860	173	83	90	19.5	1.06	20.68	0.98	19.70	5.62	0.750	134	2.128
G-12	20.0	0.5050	174	84	90	22.5	1.23	27.68	0.98	26.70	7.60	0.881	176	2.246
G-13	19.85	0.6420	178	86	92	25.5	1.39	35.45	1.02	34.43	9.55	0.980	220	2.342
G-14	19.35	0.9770	181	87	94	27.5	1.56	42.90	1.06	41.84	11.32	1.054	325	2.512
G-15	19.75	1.400	179	86	93	31.0	1.69	52.39	1.04	51.35	14.09	1.149	477	2.679
G-16	20.0	1.040	179	86	93	28.9	1.58	45.52	1.04	44.48	11.87	1.074	359	2.555

Table II (Cont'd)

Experimental Data for 0.25 in Diameter Cylinder

Run	f cps	2a in	t_w F	t_a F	$t_w - t_a$ F	I Amps	E Volts	EI Watts	Q_r Watts	Q_c Watts	$\frac{Nu}{Pr^{.3}}$	Log $\frac{Nu}{Pr^{.3}}$	Re	Log Re
H-1	10.17	0.6105	173	81	92	18.0	0.98	17.63	0.74	16.89	4.72	0.674	109	2.038
H-2	29.7	0.2945	176	84	92	18.0	0.98	17.63	0.75	16.88	4.69	0.671	152	2.183
H-3	29.2	0.3845	177	86	91	21.0	1.14	23.95	0.75	23.20	6.50	0.813	194	2.289
H-4	10.0	0.7450	179	86	93	21.0	1.14	23.95	0.77	23.18	6.35	0.803	124	2.092

Table III

Experimental Data for 0.75 in Diameter Cylinder

Run	f cps	2a in	t_w F	t_a F	t_w-t_a F	I Amps	E Volts	EI Watts	Q_r Watts	Q_c Watts	$\frac{Nu}{Pr^{.3}}$	$\log\frac{Nu}{Pr^{.3}}$	Re	Log Re
I-1	0.0	0.0	120	70	50	22.5	0.56	12.60	0.53	12.07	6.06	0.782	0	--
I-2	48.3	0.0727	122	72	50	22.5	0.56	12.60	0.54	12.06	6.04	0.781	204	2.310
I-3	48.3	0.0838	122	72	50	22.5	0.56	12.60	0.54	12.06	6.04	0.781	236	2.372
I-4	48.3	0.1011	123	73	50	22.5	0.56	12.60	0.54	12.06	6.03	0.780	283	2.452
I-5	46.8	0.1427	123	73	50	22.5	0.56	12.60	0.54	12.06	6.03	0.780	387	2.588
I-6	43.2	0.2335	124	74	50	23.0	0.57	13.11	0.54	12.57	6.27	0.797	583	2.766
I-7	43.2	0.2890	125	75	50	26.0	0.65	16.90	0.55	16.35	8.14	0.901	720	2.857
I-8	43.2	0.3035	125	75	50	27.0	0.68	18.37	0.55	17.32	8.88	0.948	756	2.879
I-9	43.2	0.2600	125	75	50	25.0	0.62	15.50	0.55	14.95	7.44	0.872	648	2.812
I-10	43.2	0.2545	125	75	50	24.0	0.60	14.40	0.55	13.85	6.90	0.839	634	2.802
I-11	45.7	0.3060	126	76	50	28.0	0.70	19.60	0.55	19.05	9.48	0.977	804	2.906
I-12	48.6	0.3085	128	78	50	29.0	0.72	20.88	0.55	20.33	10.10	1.004	856	2.932
I-13	44.6	0.3283	130	80	50	30.0	0.75	22.50	0.56	21.94	10.86	1.036	832	2.920
I-14	44.6	0.3325	131	81	50	31.0	0.78	24.18	0.56	23.62	11.67	1.067	839	2.924
I-15	44.1	0.3590	131	81	50	32.0	0.80	25.76	0.56	25.20	12.45	1.095	893	2.951
I-16	44.3	0.3550	132	82	50	33.0	0.83	27.06	0.57	26.49	13.06	1.116	910	2.959
I-17	41.5	0.3810	134	84	50	34.0	0.86	29.24	0.57	28.67	14.10	1.149	885	2.947
I-18	42.5	0.3860	130	80	50	35.0	0.89	31.15	0.56	30.59	15.14	1.180	930	2.968
I-19	42.2	0.4165	130	80	50	36.0	0.91	32.76	0.56	32.20	15.94	1.202	996	2.998
I-20	41.8	0.4120	132	82	50	37.0	0.94	34.78	0.57	34.21	16.89	1.228	971	2.987
I-21	41.6	0.4485	132	82	50	38.0	0.96	36.48	0.57	35.91	17.70	1.248	1051	3.022
I-22	41.0	0.4960	133	83	50	39.0	0.99	38.61	0.57	38.04	18.71	1.272	1142	3.058
I-23	44.0	0.3120	122	72	50	28.0	0.70	19.60	0.54	19.06	9.54	0.980	800	2.903

Table III (Cont'd)

Experimental Data for 0.75 in Diameter Cylinder

Run	f cps	2a in	t_w F	t_a F	$t_w - t_a$ F	I Amps	E Volts	EI Watts	Q_r Watts	Q_c Watts	$\frac{Nu}{Pr^{.3}}$	Log $\frac{Nu}{Pr^{.3}}$	Re	Log Re
I-24	43.9	0.3245	125	75	50	29.0	0.72	20.88	0.55	20.33	20.33	1.006	822	2.915
I-25	41.0	0.4310	130	80	50	36.0	0.91	32.76	0.56	32.20	15.93	1.202	1024	3.010
I-26	41.0	0.4420	131	81	50	37.0	0.94	34.78	0.56	34.22	16.89	1.228	1047	3.020
I-27	43.2	0.4760	132	82	50	39.0	0.99	38.61	0.56	38.05	18.77	1.273	1157	3.063
I-28	43.2	0.5215	131	82	49	41.0	1.04	42.64	0.55	42.09	21.20	1.326	1272	3.104
I-29	43.25	0.5460	133	84	49	43.0	1.10	47.30	0.56	46.74	23.50	1.371	1324	3.122
I-30	43.25	0.5605	135	85	50	45.0	1.15	51.75	0.57	51.18	25.10	1.398	1353	3.131
I-31	43.25	0.6140	135	85	50	47.0	1.20	56.40	0.57	55.83	27.40	1.438	1481	3.171
I-32	43.2	0.6430	137	87	50	49.0	1.26	61.74	0.58	61.16	29.90	1.476	1539	3.187
I-33	43.2	0.6960	139	88	51	51.0	1.31	66.81	0.60	66.81	31.70	1.501	1659	3.220
I-34	43.2	0.7510	140	88	52	53.0	1.36	72.08	0.61	71.47	33.50	1.525	1782	3.251
I-35	43.0	0.7740	141	89	52	54.0	1.38	74.52	0.61	73.91	34.60	1.539	1827	3.262
J-1	0.0	0.0	173	73	100	34.0	0.86	29.24	1.24	28.00	6.75	0.829	0	--
J-2	49.1	0.0679	174	74	100	34.0	0.86	29.24	1.24	28.00	6.72	0.827	178	2.250
J-3	48.8	0.1340	175	75	100	34.0	0.86	29.24	1.25	27.99	6.72	0.827	347	2.540
J-4	45.4	0.2195	177	75	102	34.0	0.86	29.24	1.28	29.24	6.70	0.826	528	2.723
J-5	45.1	0.2605	177	77	100	36.0	0.92	33.12	1.27	31.85	7.63	0.883	621	2.793
J-6	44.5	0.2930	178	78	100	39.0	1.00	39.00	1.27	38.73	9.25	0.966	690	2.839
J-7	43.8	0.3290	180	80	100	42.0	1.09	45.78	1.28	44.50	10.10	1.004	755	2.878
J-8	43.5	0.3740	179	81	98	45.0	1.17	52.65	1.25	51.40	12.50	1.097	852	2.930
J-9	42.1	0.3650	179	77	102	45.0	1.17	52.65	1.29	51.36	12.02	1.080	810	2.908
J-10	42.2	0.4040	180	79	101	48.0	1.25	60.00	1.29	58.71	13.88	1.142	894	2.951

Table III (Cont'd)

Experimental Data for 0.75 in Diameter Cylinder

Run	f cps	2a in	t_w F	t_a F	t_w-t_a F	I Amps	E Volts	EI Watts	Q_r Watts	Q_c Watts	$\frac{Nu}{Pr^{.3}}$	Log $\frac{Nu}{Pr^{.3}}$	Re	Log Re
J-11	42.8	0.4400	181	81	100	51.0	1.33	67.83	1.28	66.55	15.85	1.200	983	2.993
J-12	43.1	0.4610	185	85	100	54.0	1.42	76.68	1.31	75.37	17.83	1.251	1025	3.011
J-13	43.1	0.4880	184	84	100	57.0	1.49	84.93	1.30	83.63	19.82	1.297	1072	3.030

Bibliography

1. Eckert, E. R. G., and R. M. Drake, Jr. Heat and Mass Transfer (Second Edition). New York, New York: McGraw-Hill Book Co., Inc. 1959.

2. McAdams, W. H., Heat Transmission (Third Edition) New York, New York: McGraw-Hill Book Co., Inc. 1954.

3. Watson, W. J., Effect of Vibration on Heat Transfer from Cylinders Vibrated Sinusoidally within a Vertical Plane in Free Convection. Thesis (unpublished). Dayton, Ohio: Air Force Institute of Technology, December 1965.

Vita

Major Leon H. Chaffee was born [redacted] Following his graduation in 1952 from Hobart College, Geneva, New York, he received a direct commission as a Second Lieutenant in the United States Air Force and entered electronic warfare training. Upon completion of training, he was assigned to duty with the Alaskan Air Command at Elmendorf Air Force Base, Alaska. After a two year tour of duty in Alaska, he was assigned to tours of duty with the Strategic Air Command at Plattsburgh Air Force Base, New York, and Westover Air Force Base, Massachusetts, respectively. Subsequently, he entered resident training for Aerospace Mechanical Engineering (Undergraduate and then Graduate) at Wright-Patterson Air Force Base, Ohio.

Permanent Address: [redacted]

This thesis was typed by Mrs. Betty L. Lavender.